



for geotechnics & structures

CONCRETE STRUCTURES SUBJECT TO ELEVATED TEMPERATURES

Report 160102

A. Truty

GeoDev.

PO Box CH-1001 Lausanne
Switzerland
<https://zsoil.com>

Contents

1	Introduction	5
2	Thermal analysis of structures subject to elevated temperatures	7
2.1	Problem statement	7
2.2	Evolution functions for thermal properties of concrete	9
2.3	Generating radiation/convection elements	15
3	1D elasto-plastic model for steel reinforcement subject to elevated temperatures	19
3.1	Uniaxial stress-strain relations	19
3.2	Evolution functions for mechanical properties of steel reinforcement	21
4	Extension of the plastic damage model to handle fire problems	27
4.1	Thermal evolution functions for mechanical properties of concrete	28
4.2	Transient creep	36
5	Benchmarks	39
5.1	Truss element in displacement driven tensile test at elevated temperatures	39
5.1.1	Thermal analysis	40
5.1.2	Mechanical analysis	40
5.2	Displacement driven uniaxial compression test of plain concrete at elevated temperatures	42
5.2.1	Thermal analysis	43
5.2.2	Mechanical analysis	43
5.3	Anderberg and Thelandersson test	47
5.3.1	Thermal analysis	48
5.3.2	Mechanical analysis	48
5.4	Slab subject to fire conditions (Lim and Wade test)	49
5.4.1	Thermal analysis	50

CONTENTS

5.4.2 Mechanical analysis 51

5.5 Slab subject to fire conditions (Minne and Vandamme test) 54

5.5.1 Thermal analysis 55

5.5.2 Mechanical analysis 55

Chapter 1

Introduction

This report concerns a weakly coupled thermo-mechanical analysis of RC structures subject to elevated temperatures (fire). In ZSoil 2018, fire analysis, as far as structures are concerned, can be carried out using continuum, shells (with smeared reinforcement) and truss/cable finite elements exclusively. The modified Lee-Fenves plastic damage model is the only one that can be used to represent concrete behavior subject to elevated temperatures. (see [1]). Most of the evolution functions describing temperature dependent stiffness, strength and thermal properties of concrete and steel reinforcement are taken after recommendations of the Eurocode 2 and associated standards concerning fire analysis. Some missing functions are introduced based on the current literature of the matter.

Chapter 2

Thermal analysis of structures subject to elevated temperatures

2.1 Problem statement

The list of symbols used in the transient heat analyses of RC structures subject to fire conditions is given in Win.2-1.

Window 2-1: List of symbols

ZSoil®

Table 2.1: Symbols used in thermal analysis

Symbol	Quantity	Unit
Θ	temperature	[K]
t	time	[s]
λ_c	heat conductivity of concrete	[W/(m K)]
c_c	specific heat of concrete	[J/(kg K)]
ρ_c	concrete mass density	[kg/m ³]
$c_c^* = c_c \rho$	concrete heat capacity	[J/(K m ³)]
\bar{q}	external heat flux	[W/(m ²)]
Θ_g	gas temperature	[K]
Θ_r	radiation temperature	[K]
h_c	heat convection coefficient	[W/(m ² K)]
Φ	configuration coefficient	[-]
ε_m	emissivity of element surface	[-]
ε_f	fire emissivity	[-]
σ	Boltzmann constant (5.67 10 ⁻⁸)	[W/(m ² K ⁴)]

The transient heat problem, described by the nonlinear Fourier equation, supplied by appropriate boundary and initial conditions, is given in Win.2-2.

Window 2-2: Nonlinear heat transfer analysis

ZSoil®

• **Nonlinear Fourier equation (transient case):**

$$\lambda_c(\Theta) \mathbf{div grad}(\Theta) = c^*(\Theta) \frac{\partial \Theta}{\partial t} \quad \text{on } \Omega$$

In the above equation heat conductivity and capacity are explicit functions of current temperature, defined in the Eurocode separately for each concrete aggregate.

• **Boundary conditions:**

Temperature BC

with prescribed temperature $\bar{\theta}$ $\Theta = \bar{\theta}$ on Γ_θ

Heat flux BC

with prescribed heat flux \bar{q} $\lambda_c \frac{\partial \Theta}{\partial n} = -\bar{q}$ on Γ_q

Convective+radiative flux BC

$$\lambda_c \frac{\partial \Theta}{\partial n} = -h_c (\Theta - \Theta_g) - \Phi \varepsilon_m \varepsilon_f \sigma ((\Theta + 273)^4 - (\Theta_r + 273)^4) \quad \text{on } \Gamma_c$$

Note: $(\Gamma_q \cup \Gamma_c) \cup \Gamma_T = \Gamma$; but $(\Gamma_q \cup \Gamma_c) \cap \Gamma_T = \emptyset$

For elements fully subject to fire one may assume $\Theta_g = \Theta_r$.

Time history of gas temperature can be described by so-called standard curve

$\Theta_g(t) = 20 + 345 \log_{10}(8t + 1)$ (time in [min]).

• **Initial conditions:**

Known temperature field Θ_0 at time $t = 0$: $\Theta(\mathbf{x}, 0) = \Theta_0(\mathbf{x})$ in Ω

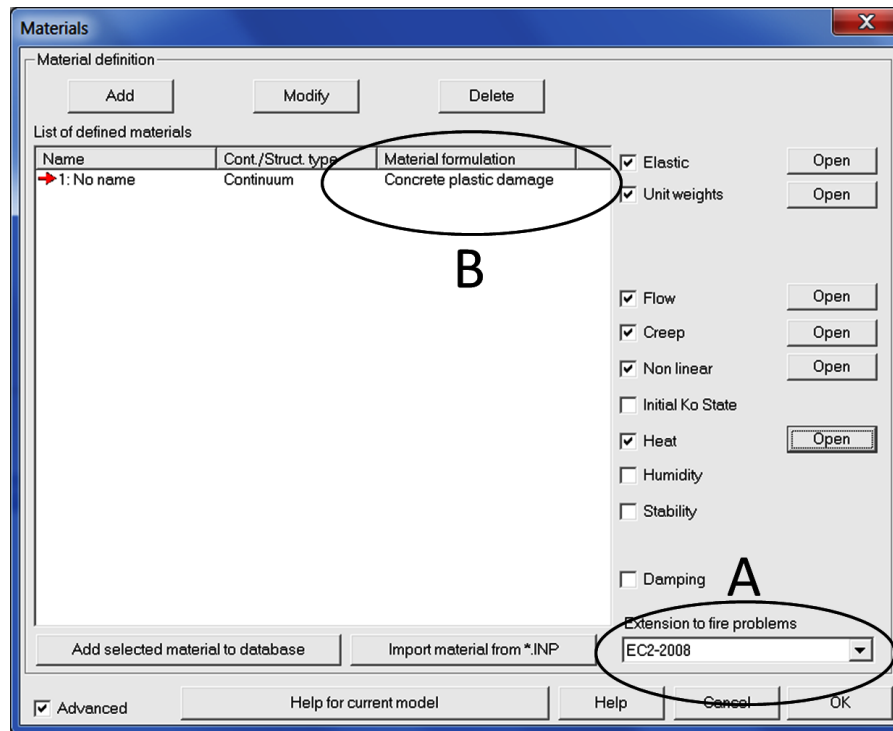
Window 2-2

2.2 Evolution functions for thermal properties of concrete

The plastic damage model for concrete is the only one that allows carrying out thermal analyses of concrete structures subject to fire conditions. For this model one can activate fire extensions (see Win.2-3) compatible with the Eurocode standard (2008).

Window 2-3: Activating fire extensions in plastic damage model

ZSoil®



Remarks:

- To activate fire extensions, option EC2-2008 must be selected in the combo box (A)
- For any other model for continuum this combo-box is invisible

Window 2-3

CHAPTER 2. THERMAL ANALYSIS OF STRUCTURES SUBJECT TO ELEVATED TEMPERATURES

Three parameters ie. heat conductivity λ_c , heat capacity c^* and thermal solid dilatancy α_c vary with temperature following the explicit functions given in the Eurocode 2. Values of these parameters vary with temperature according to the specified thermal evolution functions. Notion of these functions is explained in Win.2-4.

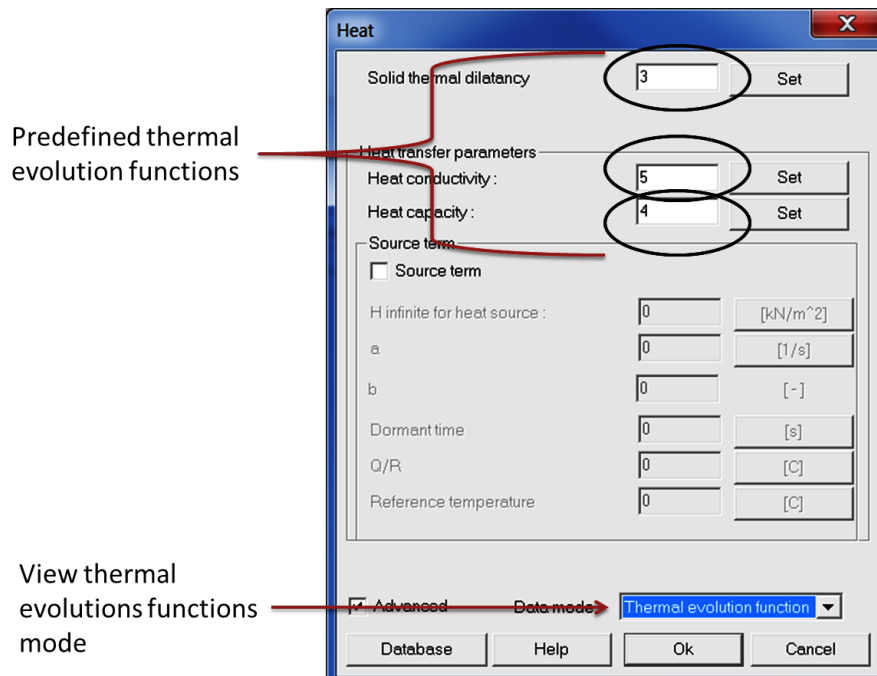
Window 2-4: Notion of evolution functions for selected thermal properties

ZSoil®

Thermal evolution functions for heat conductivity λ_c , heat capacity c^* and thermal solid dilatancy α_c are defined as follows:

$$k_{\lambda_c}(\Theta) = \frac{\lambda_c(\Theta)}{\lambda_c(\Theta = 20^\circ \text{C})}$$
$$k_{c^*}(\Theta) = \frac{c^*(\Theta)}{c^*(\Theta = 20^\circ \text{C})}$$
$$k_{\alpha_c}(\Theta) = \frac{\alpha_c(\Theta)}{\alpha_c(\Theta = 20^\circ \text{C})}$$

In the dialog box for the material data (under standard input mode) user sets reference values of these parameters ie. at assumed temperature $\Theta = 20^\circ \text{C}$. By switching the input mode to the thermal evolutions functions (see fig.below), once the fire extension is activated, three predefined functions (based on EC-2) k_{λ_c} , k_{c^*} and k_{α_c} are set.



Window 2-4

Window 2-5: Evolution function $k_{\lambda_c}(\Theta)$

ZSoil®

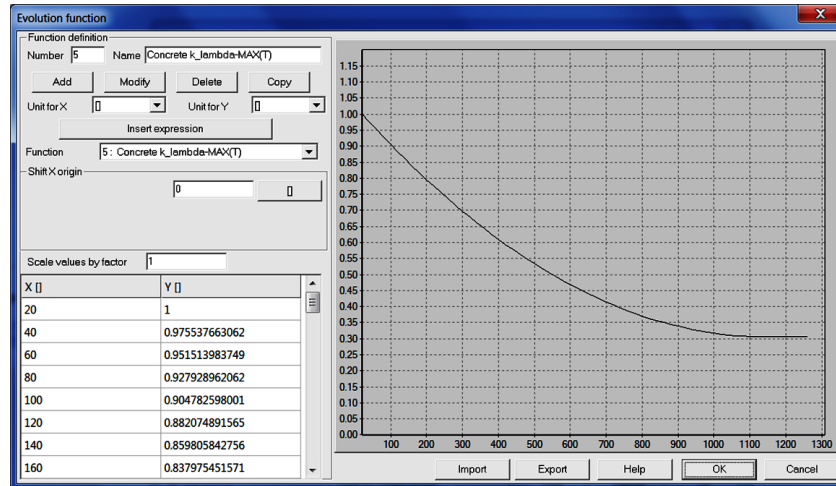
Upper limit of heat conductivity (recommended by the EC2)

$$\lambda_c^{\max}(\Theta) = 2 - 0.2451 (\Theta/100) + 0.0107 (\Theta/100)^2 \text{ [W/mK] for } 20^\circ\text{C} \leq \Theta \leq 1200^\circ\text{C}.$$

Hence

$$k_{\lambda_c^{\max}}(\Theta) = \frac{\lambda_c^{\max}(\Theta)}{\lambda_c^{\max}(\Theta = 20^\circ\text{C})} \text{ and } \lambda_c^{\max}(\Theta = 20^\circ\text{C}) = 1.951 \text{ [W/mK]}.$$

This function is shown in the following figure



NB. $\lambda_c^{\max}(\Theta = 20^\circ\text{C}) = 1.9514 \text{ W/mK}$

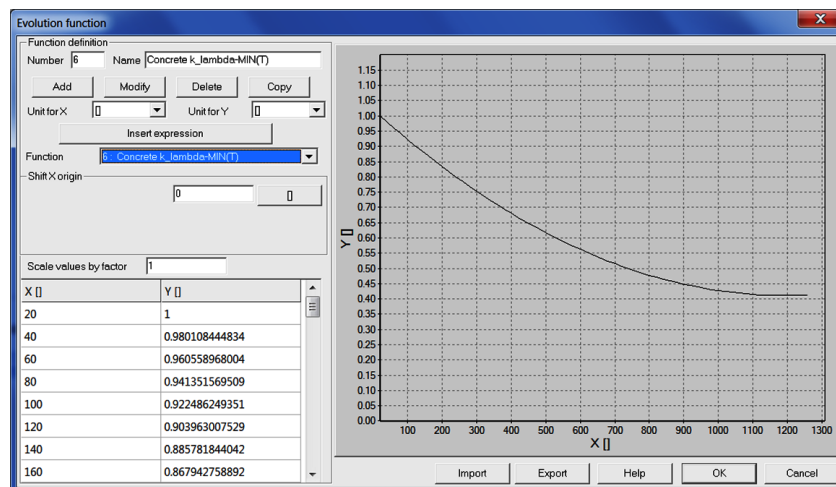
Lower limit of heat conductivity

$$\lambda_c^{\min}(\Theta) = 1.36 - 0.136 (\Theta/100) + 0.0057 (\Theta/100)^2 \text{ [W/mK] for } 20^\circ\text{C} \leq \Theta \leq 1200^\circ\text{C}.$$

Hence

$$k_{\lambda_c^{\min}}(\Theta) = \frac{\lambda_c^{\min}(\Theta)}{\lambda_c^{\min}(\Theta = 20^\circ\text{C})} \text{ and } \lambda_c^{\min}(\Theta = 20^\circ\text{C}) = 1.333 \text{ [W/mK]}.$$

This function is shown in the following figure



NB. $\lambda_c^{\min}(\Theta = 20^\circ\text{C}) = 1.333 \text{ W/mK}$

Window 2-5

Window 2-6: Evolution function $k_{c^*}(\Theta)$

ZSoil®

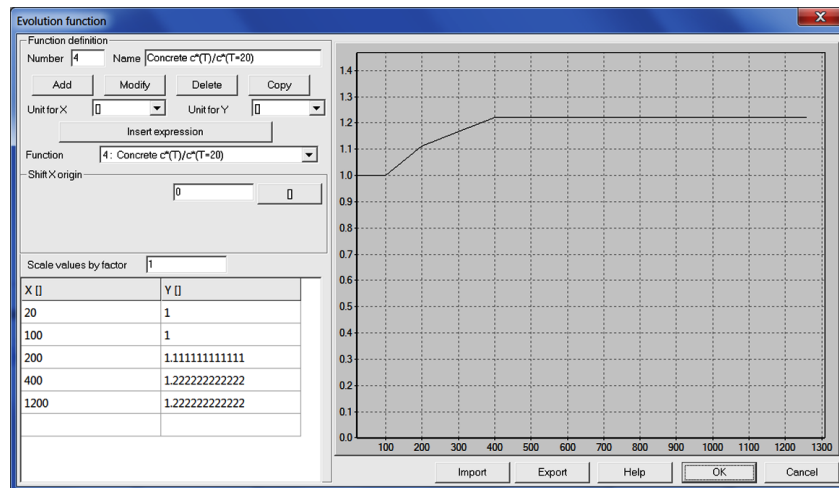
Specific heat of dry concrete c_c

$$\begin{aligned} c_c &= 900 & [\text{J/kg K}] & \text{for } 20^\circ\text{C} \leq \Theta \leq 100^\circ\text{C} \\ c_c &= 900 + (\Theta - 100) & [\text{J/kg K}] & \text{for } 100^\circ\text{C} \leq \Theta \leq 200^\circ\text{C} \\ c_c &= 1000 + (\Theta - 200)/2 & [\text{J/kg K}] & \text{for } 200^\circ\text{C} \leq \Theta \leq 400^\circ\text{C} \\ c_c &= 1100 & [\text{J/kg K}] & \text{for } 400^\circ\text{C} \leq \Theta \leq 1200^\circ\text{C} \end{aligned}$$

Here we assume that

$$k_{c^*}(\Theta) = k_{c_c}(\Theta) = \frac{c_c(\Theta)}{c_c(\Theta = 20^\circ\text{C})} = \frac{c_c^*(\Theta)}{c_c^*(\Theta = 20^\circ\text{C})}.$$

This function is shown in the following figure.



NB. $c_c^*(\Theta = 20^\circ\text{C}) = c_c \rho_c = 0.9 \text{ kJ/kg K} \cdot 2400 \text{ kg/m}^3 = 2160 \text{ kJ/m}^3 \text{ K}$

Remarks:

1. $c_c \approx 2000 \text{ [J/kgK]}$ for humidity content equal to 3% of concrete weight (standard situation); this yields $c_c^*(\Theta = 20^\circ\text{C}) = c_c \rho_c = 2.0 \text{ kJ/kg K} \cdot 2400 \text{ kg/m}^3 = 4800 \text{ kJ/m}^3 \text{ K}$
2. $c_c \approx 5500 \text{ [J/kgK]}$ for humidity content equal to 10% of concrete weight; this yields $c_c^*(\Theta = 20^\circ\text{C}) = c_c \rho_c = 5.5 \text{ kJ/kg K} \cdot 2400 \text{ kg/m}^3 = 13200 \text{ kJ/m}^3 \text{ K}$

Window 2-6

Window 2-7: Evolution function $k_{\alpha_c}(\Theta)$ for siliceous aggregate

ZSoil®

Thermal expansion $\Delta l/l$:

$$\begin{aligned}\Delta l/l &= -1.8 \cdot 10^{-4} + 9.1 \cdot 10^{-6} \Theta + 2.3 \cdot 10^{-11} \Theta^3 & \text{for } 20^\circ\text{C} \leq \Theta \leq 700^\circ\text{C} \\ \Delta l/l &= 14.1 \cdot 10^{-3} & \text{for } 700^\circ\text{C} \leq \Theta \leq 1200^\circ\text{C}\end{aligned}$$

Parameter α_c is derived using the following formula:

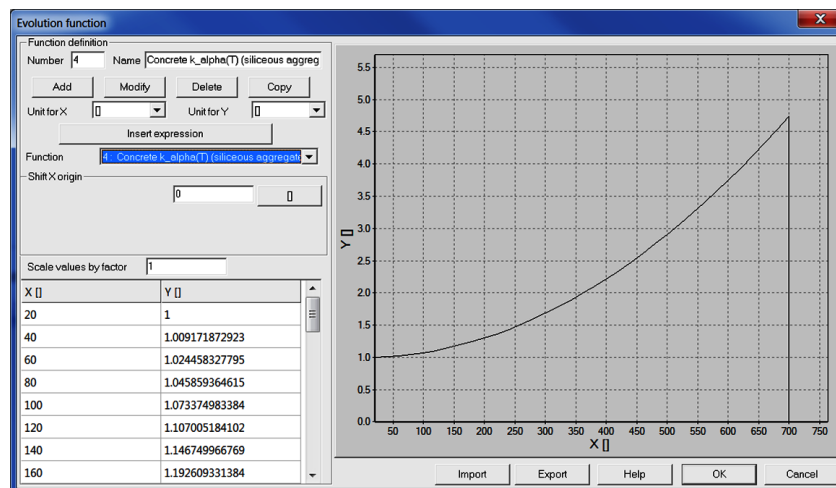
$$\alpha_c(\Theta) = \frac{d(\Delta l/l(\Theta))}{d\Theta}$$

This yields:

$$\begin{aligned}\alpha_c(\Theta) &= 9.1 \cdot 10^{-6} + 6.9 \cdot 10^{-11} \Theta^2 & \text{for } 20^\circ\text{C} \leq \Theta \leq 700^\circ\text{C} \\ \alpha_c(\Theta) &= 0.0 & \text{for } 700^\circ\text{C} \leq \Theta \leq 1200^\circ\text{C}\end{aligned}$$

Hence

$$k_\alpha(\Theta) = \frac{\alpha_c(\Theta)}{\alpha_c(\Theta = 20^\circ\text{C})}$$



Remarks:

$$1. \alpha_c(\Theta = 20^\circ\text{C}) = 9.128 \cdot 10^{-6}$$

Window 2-7

Window 2-8: Evolution function $k_{\alpha_c}(\Theta)$ for calcareous aggregate

ZSoil®

Thermal expansion $\Delta l/l$:

$$\begin{aligned}\Delta l/l &= -1.2 \cdot 10^{-4} + 6 \cdot 10^{-6} \Theta + 1.4 \cdot 10^{-11} \Theta^3 & \text{for } 20^\circ\text{C} \leq \Theta \leq 805^\circ\text{C} \\ \Delta l/l &= 12 \cdot 10^{-3} & \text{for } 805^\circ\text{C} \leq \Theta \leq 1200^\circ\text{C}\end{aligned}$$

Parameter α_c is derived using the following formula:

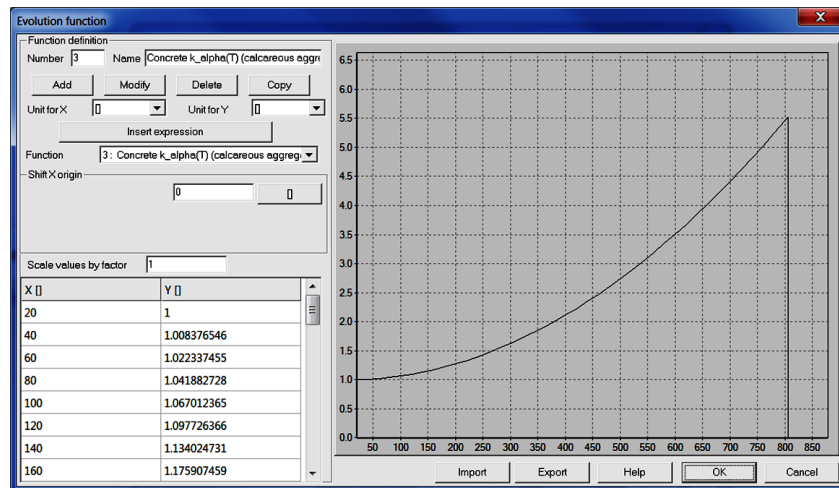
$$\alpha_c(\Theta) = \frac{d(\Delta l/l(\Theta))}{d\Theta}$$

This yields:

$$\begin{aligned}\alpha_c(\Theta) &= 6 \cdot 10^{-6} + 4.2 \cdot 10^{-11} \Theta^2 & \text{for } 20^\circ\text{C} \leq \Theta \leq 805^\circ\text{C} \\ \alpha_c(\Theta) &= 0.0 & \text{for } 805^\circ\text{C} \leq \Theta \leq 1200^\circ\text{C}\end{aligned}$$

Hence

$$k_\alpha(\Theta) = \frac{\alpha_c(\Theta)}{\alpha_c(\Theta = 20^\circ\text{C})}$$



Remarks:

$$1. \alpha_c(\Theta = 20^\circ\text{C}) = 6.017 \cdot 10^{-6}$$

Window 2-8

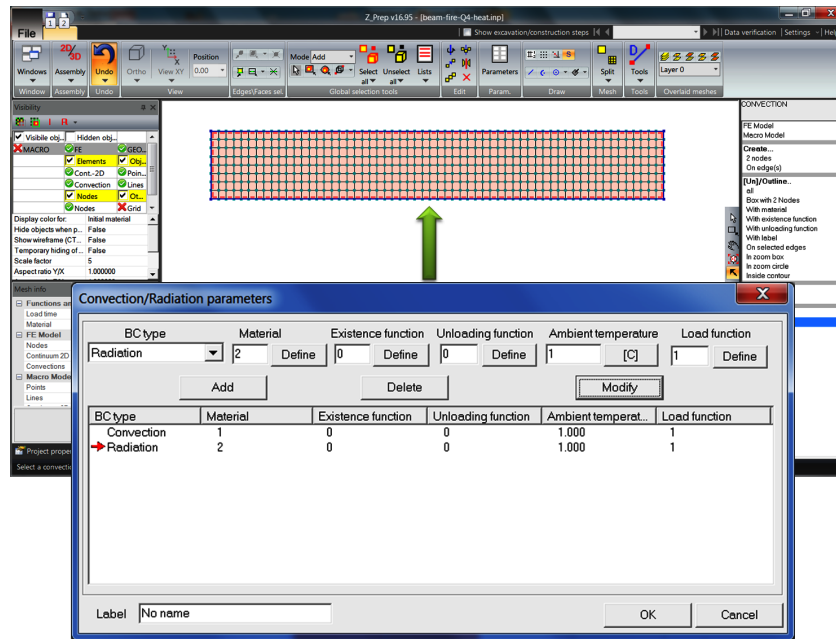
2.3 Generating radiation/convection elements

Convection and radiation elements can simultaneously be added to the mesh boundary in the preprocessing stage. Example of radiation/convection elements generation is shown in Win.2-9.

Window 2-9: Generating convection/radiation boundaries

ZSoil®

Convection and/or radiation elements simulate convective/radiation boundary condition.



Remarks:

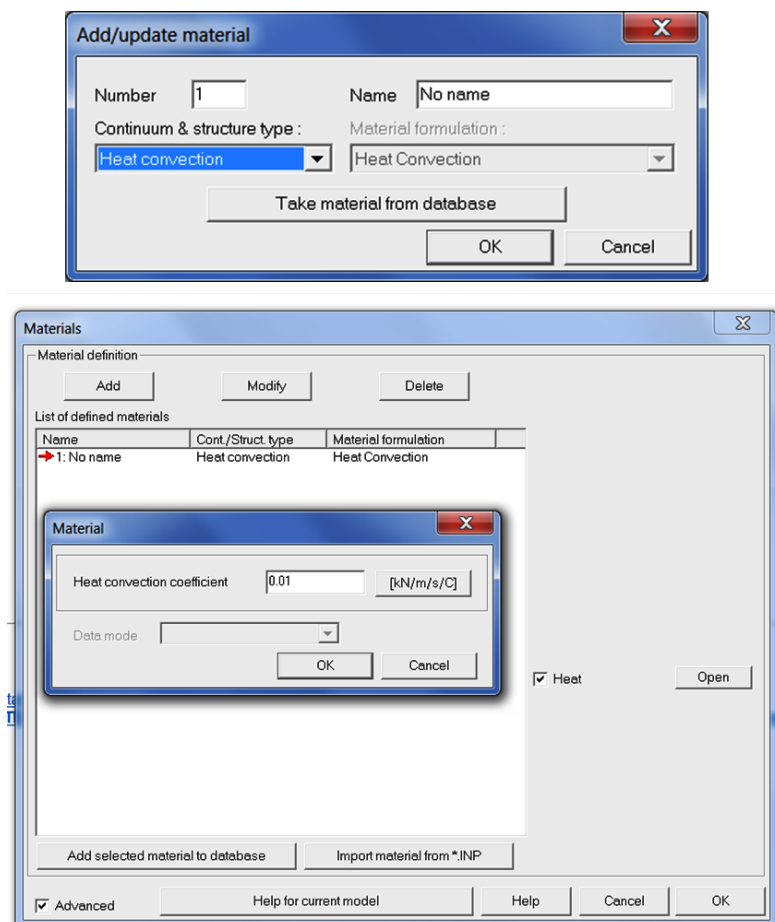
1. Material numbers for convection and radiation elements are different (different material data is required)
2. Ambient temperature in case of convective boundary is understood as $\Theta_g(t)$
3. Ambient temperature in case of radiation boundary is understood as $\Theta_r(t)$
4. The $\Theta_g(t)$ function can be defined as (time in [min], temperature in °C):
 - A: Standard curve: $\Theta_g(t) = 20 + 345 \log_{10}(8t + 1)$ ($h_c=25$ [W/m²K])
 - B: External fire curve: $\Theta_g(t) = 660 (1 - 0.687 e^{-0.32t} - 0.313 e^{-3.8t}) + 20$ ($h_c=25$ [W/m²K])
 - C: Hydrocarbon curve: $\Theta_g(t) = 1080 (1 - 0.325 e^{-0.167t} - 0.675 e^{-2.5t}) + 20$ ($h_c=50$ [W/m²K])

Window 2-9

Window 2-10: Material data for convective boundary

ZSoil®

In case of convection elements set of material properties consists of a single parameter ie. convection coefficient h_c that is assumed as constant.



Remarks:

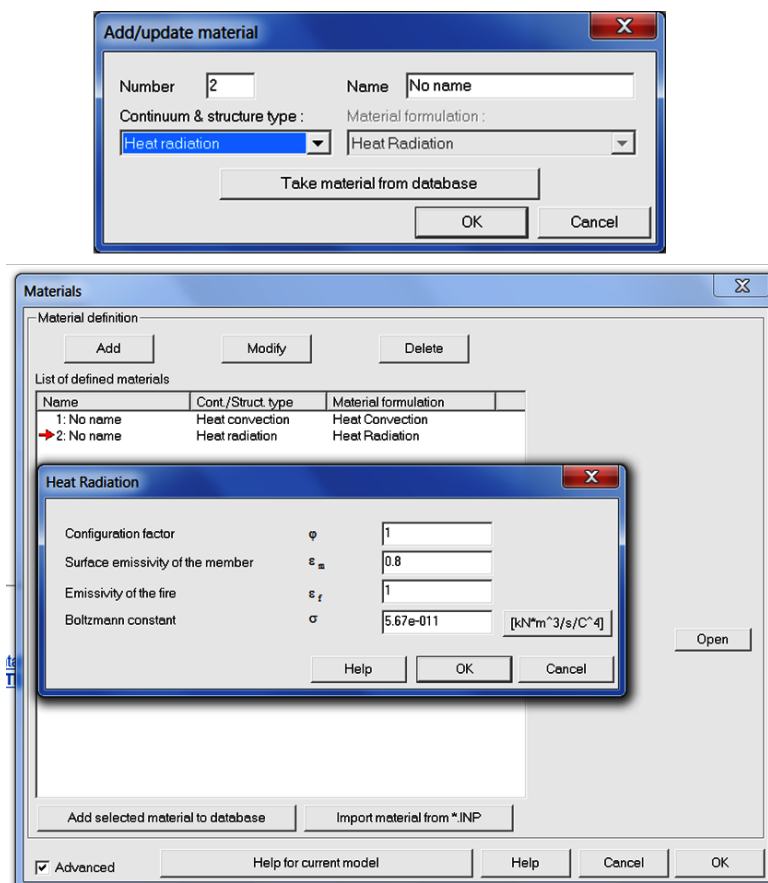
1. For standard curve $\Theta_g(t)$ (see Win.2-9 for definition) : $h_c=25$ [W/m²K]
2. For external fire curve $\Theta_g(t)$ (see Win.2-9 for definition): $h_c=25$ [W/m²K]
3. For hydrocarbon curve $\Theta_g(t)$ (see Win.2-9 for definition): $h_c=50$ [W/m²K]

Window 2-10

Window 2-11: Material data for radiation boundary

ZSoil®

In case of radiation elements set of material properties consists of four parameters ie. configuration factor Φ , surface emissivity of the member ε_m , emissivity of the fire ε_f and Stefan Boltzmann constant σ .

**Remarks:**

1. The recommended value for configuration factor $\Phi = 1.0$; this value can be lower when shadow or location effects are analyzed; for more detailed setup see the EC2 standard
2. The recommended value for surface emissivity of the member is $\varepsilon_m = 0.8$
3. The recommended value for emissivity of the fire is $\varepsilon_f = 1.0$
4. Stefan Boltzmann constant is $\sigma = 5.67 \cdot 10^{-8} \text{ [W/m}^2\text{K}^4\text{]}$

Window 2-11

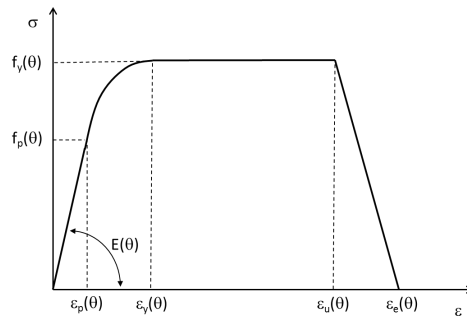
Chapter 3

1D elasto-plastic model for steel reinforcement subject to elevated temperatures

3.1 Uniaxial stress-strain relations

Window 3-1: Stress-strain law for steel reinforcement (EC2 model)

ZSoil®



The uniaxial stress-strain law for steel reinforcement at elevated temperatures is described as follows (argument Θ is omitted for sake of simplicity)

ε	σ	Tangent E_t
$\leq \varepsilon_p$	$E \varepsilon$	E
$\varepsilon_p \leq \varepsilon \leq \varepsilon_y$	$f_p - c + \frac{b}{a} [a^2 - (\varepsilon_y - \varepsilon)^2]^{0.5}$	$\frac{b(\varepsilon_y - \varepsilon)}{a[a^2 - (\varepsilon - \varepsilon_y)^2]^{0.5}}$
$\varepsilon_y \leq \varepsilon \leq \varepsilon_u$	f_y	0
$\varepsilon_u \leq \varepsilon \leq \varepsilon_e$	$f_y \left[1 - \frac{\varepsilon - \varepsilon_u}{\varepsilon_e - \varepsilon_u} \right]$	$-\frac{f_y}{\varepsilon_e - \varepsilon_u}$
$\varepsilon_e \leq \varepsilon$	0	0

where:

$$a^2 = (\varepsilon_y - \varepsilon_p)(\varepsilon_y - \varepsilon_p + c/E), \quad b^2 = c(\varepsilon_y - \varepsilon_p)E + c^2, \quad c = \frac{(f_y - f_p)^2}{(\varepsilon_y - \varepsilon_p)E - 2(f_y - f_p)}$$

$$\varepsilon_p = f_p/E, \quad \varepsilon_y = 0.02, \quad \varepsilon_u = 0.15, \quad \varepsilon_e = 0.20$$

Remarks:

CHAPTER 3. 1D ELASTO-PLASTIC MODEL FOR STEEL REINFORCEMENT SUBJECT TO ELEVATED TEMPERATURES

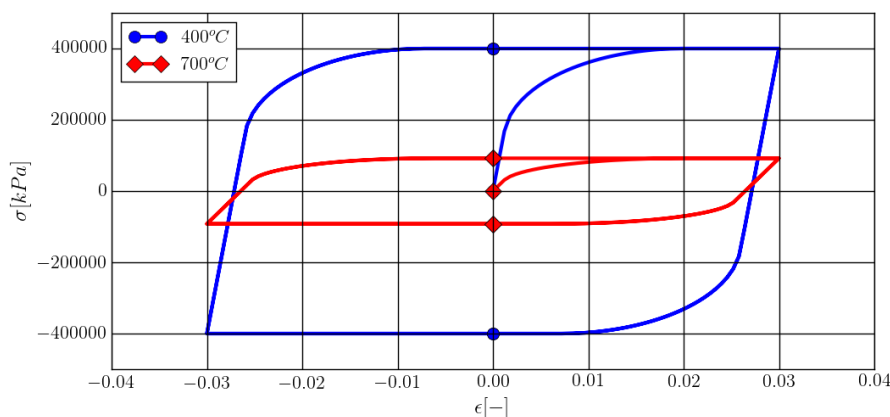
1. The above model is limited to the monotonic loading

Window 3-1

Window 3-2: Elasto-plastic model formulation

ZSoil®

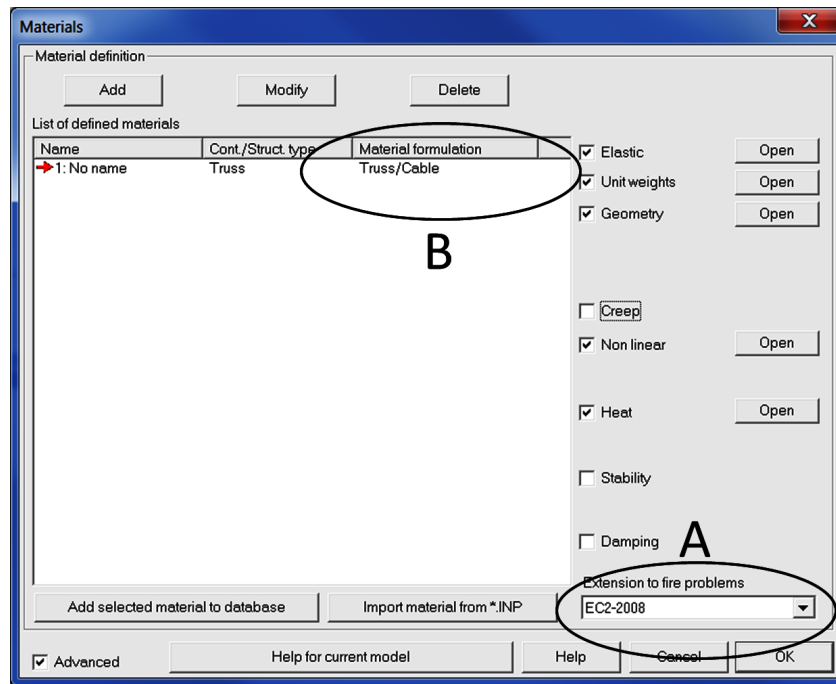
The uniaxial stress-strain law described in Win.3-1 is implemented in the framework of elasto-plasticity with hardening/softening. Behavior of the model in cyclic test is shown in the figure.



- Yield surface: $f(\sigma) = |\sigma| - \tilde{f}_y(\tilde{\varepsilon}) = 0$
- Flow rule: $g(\sigma) = f(\sigma)$
- Hardening rule: $\tilde{\varepsilon} = \max(\tilde{\varepsilon}^+, \tilde{\varepsilon}^-)$
 where (plastic strains are denoted by ε^p):
 $\tilde{\varepsilon}^+ = \varepsilon^{p+} + \frac{\sigma}{E}$ for tensile stresses
 $\tilde{\varepsilon}^- = -(\varepsilon^{p-} + \frac{\sigma}{E})$ for compressive stresses
 ε^{p-} is the accumulated compressive plastic strain
 ε^{p+} is the accumulated tensile plastic strain
 $\tilde{f}_y(\tilde{\varepsilon}) = f_p$ for $\tilde{\varepsilon} \leq \varepsilon_p$
 $\tilde{f}_y(\tilde{\varepsilon}) = \sigma$ for $\tilde{\varepsilon} > \varepsilon_p$ (see second column with σ values in table in Win.3-1)

Window 3-2

ZSoil®



- To activate fire extensions, option EC2-2008 must be selected in the combo box (**A**)
- This model can exclusively be associated with truss elements and shell fiber type reinforcement

Four parameters ie. Young's modulus E , compressive/tensile strength f_y , initial strength ratio f_p/f_y and thermal solid dilatancy α_s vary with temperature following the explicit functions given in the Eurocode 2. Values of these parameters vary with temperature according to the specified thermal evolution functions. Notion of these functions is explained in Win.3-4.

Window 3-4: Notion of evolution functions for selected mechanical properties

ZSoil®

Thermal evolution functions for Young's modulus E , compressive/tensile strength f_y , initial strength ratio f_p/f_y and thermal solid dilatancy α_s are defined as follows:

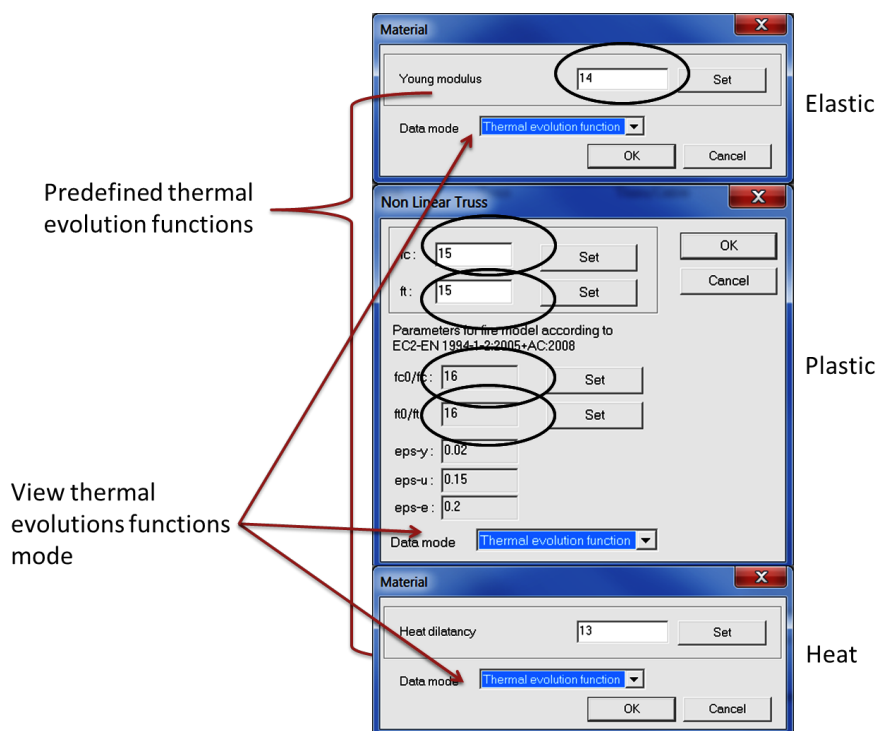
$$k_E(\Theta) = \frac{E(\Theta)}{E(\Theta = 20^\circ \text{ C})}$$

$$k_p(\Theta) = \frac{f_p(\Theta)}{f_y(\Theta = 20^\circ \text{ C})}$$

$$k_y(\Theta) = \frac{f_y(\Theta)}{f_y(\Theta = 20^\circ \text{ C})}$$

$$k_{\alpha_s}(\Theta) = \frac{\alpha_s(\Theta)}{\alpha_s(\Theta = 20^\circ \text{ C})}$$

In the dialog box for the elastic, plastic and thermal parameters (under standard input mode) user sets reference values of these parameters ie. at temperature $\Theta = 20^\circ \text{ C}$. By switching the input mode to the thermal evolutions functions (see fig.below), once the fire extension is activated, four predefined functions (based on EC-2) $k_E(\Theta)$, $k_p(\Theta)$, $k_y(\Theta)$, $k_{\alpha_s}(\Theta)$ are set.



Remarks:

1. Different reference values for the tensile and compressive stresses can be assumed in general
2. Same degradation functions are used in tension and compression
3. Steel N classes, cold-drawn and hot rolled, are supported in the current data base

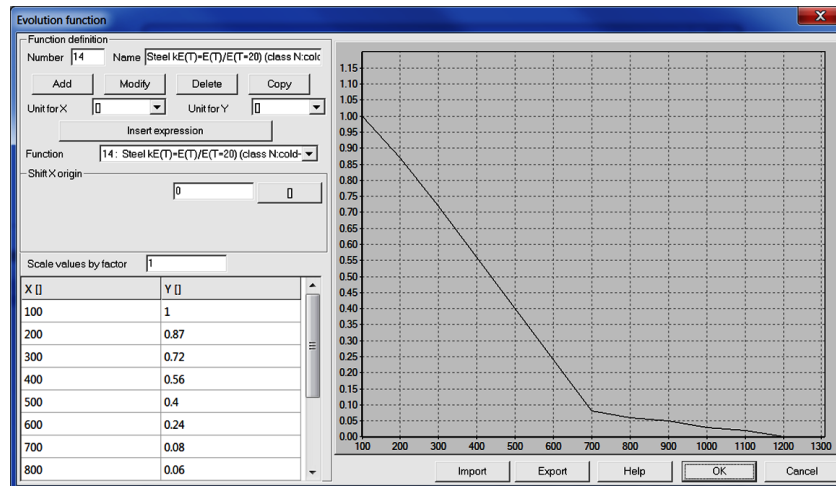
Window 3-4

3.2. EVOLUTION FUNCTIONS FOR MECHANICAL PROPERTIES OF STEEL REINFORCEMENT

Window 3-5: Evolution function $k_E(\Theta)$ for steel N (cold-drawn)

ZSoil®

The $k_E(\Theta)$ function for steel class N (cold-drawn) is shown in the following figure

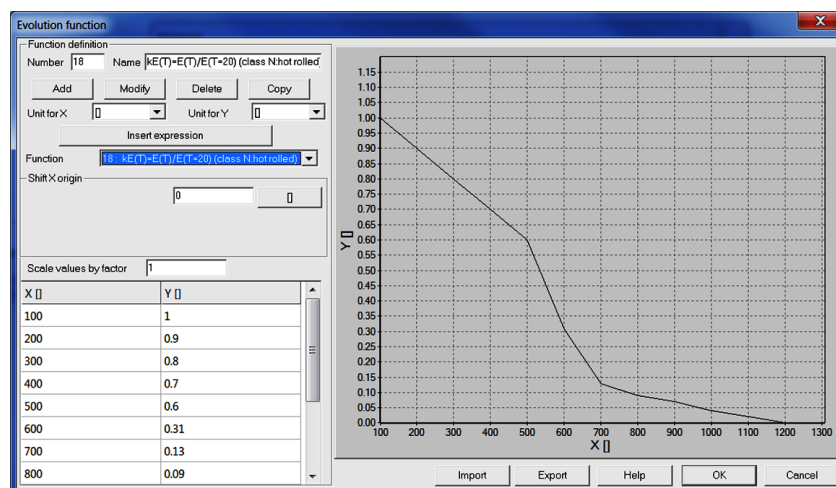


Window 3-5

Window 3-6: Evolution function $k_E(\Theta)$ for steel N (hot-rolled)

ZSoil®

The $k_E(\Theta)$ function for steel class N (hot-rolled) is shown in the following figure

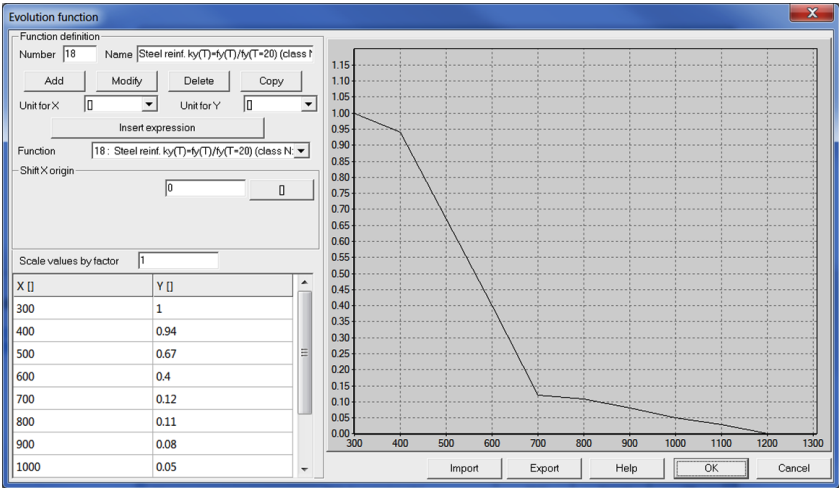


Window 3-6

Window 3-7: Evolution function $k_y(\Theta)$ for steel N (cold-drawn)

ZSoil®

The $k_y(\Theta)$ function for steel class N (cold-drawn) is shown in the following figure

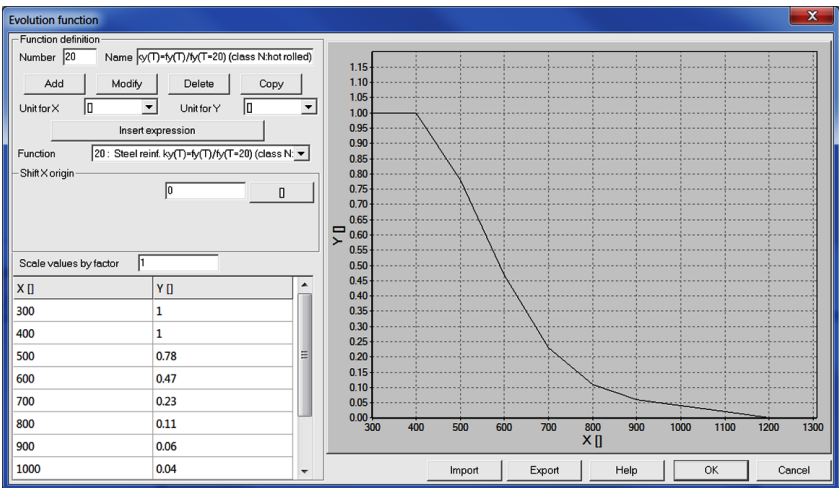


Window 3-7

Window 3-8: Evolution function $k_y(\Theta)$ for steel N (hot-rolled)

ZSoil®

The $k_y(\Theta)$ function for steel class N (hot-rolled) is shown in the following figure



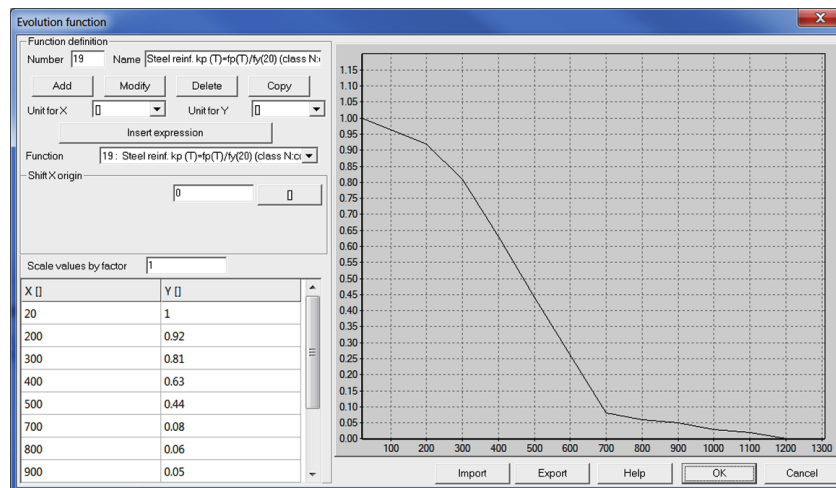
Window 3-8

3.2. EVOLUTION FUNCTIONS FOR MECHANICAL PROPERTIES OF STEEL REINFORCEMENT

Window 3-9: Evolution function $k_p(\Theta)$ for steel N (cold-drawn)

ZSoil®

The $k_p(\Theta)$ function for steel class N (cold-drawn) is shown in the following figure

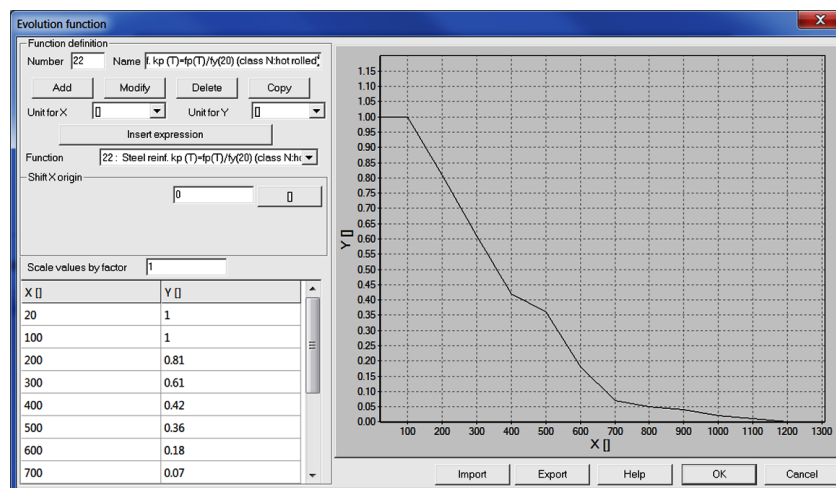


Window 3-9

Window 3-10: Evolution function $k_p(\Theta)$ for steel N (hot-rolled)

ZSoil®

The $k_p(\Theta)$ function for steel class N (hot-rolled) is shown in the following figure



Window 3-10

CHAPTER 3. 1D ELASTO-PLASTIC MODEL FOR STEEL REINFORCEMENT SUBJECT TO ELEVATED TEMPERATURES

Window 3-11: Evolution function $k_{\alpha_s}(\Theta)$

ZSoil®

Thermal expansion $\Delta l/l$:

$$\begin{aligned}\Delta l/l &= -2.416 \cdot 10^{-4} + 1.2 \cdot 10^{-5} \Theta + 0.4 \cdot 10^{-8} \Theta^2 & \text{for } 20^\circ\text{C} \leq \Theta \leq 750^\circ\text{C} \\ \Delta l/l &= 11 \cdot 10^{-3} & \text{for } 750^\circ\text{C} \leq \Theta \leq 860^\circ\text{C} \\ \Delta l/l &= -6.2 \cdot 10^{-3} + 2 \cdot 10^{-5} \Theta & \text{for } 860^\circ\text{C} \leq \Theta \leq 1200^\circ\text{C}\end{aligned}$$

Parameter α_c is derived using the following formula:

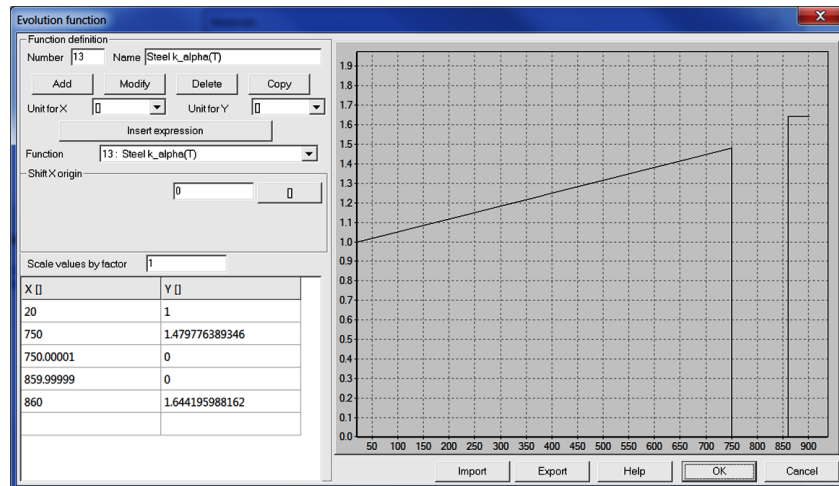
$$\alpha_s(\Theta) = \frac{d(\Delta l/l(\Theta))}{d\Theta}$$

This yields:

$$\begin{aligned}\alpha_s(\Theta) &= 1.2 \cdot 10^{-5} + 0.8 \cdot 10^{-8} \Theta & \text{for } 20^\circ\text{C} \leq \Theta \leq 750^\circ\text{C} \\ \alpha_s(\Theta) &= 0 & \text{for } 750^\circ\text{C} \leq \Theta \leq 860^\circ\text{C} \\ \alpha_s(\Theta) &= 2.0 \cdot 10^{-5} & \text{for } 860^\circ\text{C} \leq \Theta \leq 1200^\circ\text{C}\end{aligned}$$

Hence

$$k_{\alpha_s}(\Theta) = \frac{\alpha_s(\Theta)}{\alpha_s(\Theta = 20^\circ\text{C})}$$



Remarks:

$$1. \alpha_s(\Theta = 20^\circ\text{C}) = 1.216 \cdot 10^{-5}$$

Window 3-11

Chapter 4

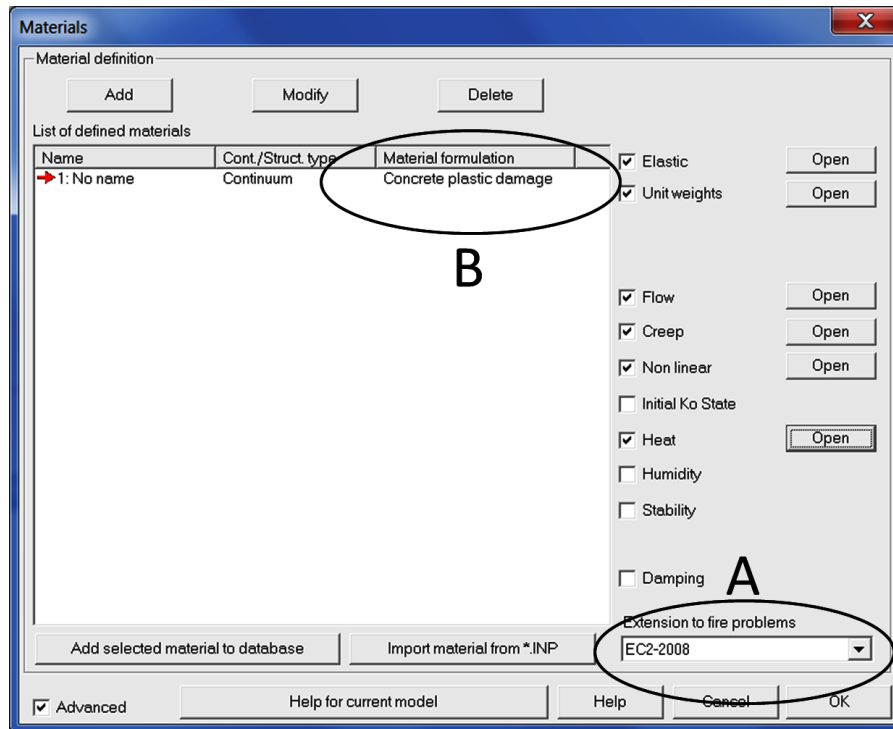
Extension of the plastic damage model to handle fire problems

Modified Lee-Fenves plastic damage model is the only one that may represent concrete behavior at elevated temperatures in the 2D/3D analyses in which structures are discretized with aid of continuum and layered shell elements. Detailed report on the standard model is given in reference [1]. In this chapter model modifications, in the context of fire conditions, are presented. Therefore this chapter of the report has to be analyzed together with the report [1].

4.1 Thermal evolution functions for mechanical properties of concrete

Window 4-1: Activating fire extensions in plastic damage model

ZSoil®



Remarks:

- To activate fire extensions, option EC2-2008 must be selected in the combo box (**A**)
- This extension is available in plastic damage model for continuum and core layer of layered (nonlinear) shells

Window 4-1

Six parameters ie. Young's modulus E , Poisson's ratio ν , compressive strength f_c , stress ratio at damage activation in compression $\sigma_{c,D}/f_c$, initial biaxial strength ratio f_{cbo}/f_{co} and tensile strength f_t are modified with aid of six independent thermal evolution functions. Certain simplifying hypotheses concerning fracture energies in tension and compression, matching damage levels \tilde{D}_c and \tilde{D}_t are proposed. Evolution function for the thermal solid dilatancy α_c is already defined in the chapter concerning thermal analyses (see Win.2-8, 2-7).

4.1. THERMAL EVOLUTION FUNCTIONS FOR MECHANICAL PROPERTIES OF CONCRETE

Window 4-2: Notion of evolution functions for selected mechanical properties

ZSoil®

Thermal evolution functions for Young modulus E , Poisson's ratio ν , compressive strength f_c , stress ratio at damage activation in compression $\sigma_{c,D}/f_c$, biaxial strength ratio f_{cb}/f_c and tensile strength f_t are defined as follows:

$$k_E(\Theta) = \frac{E(\Theta)}{E(\Theta = 20^\circ \text{ C})}$$

$$k_\nu(\Theta) = \frac{\nu(\Theta)}{\nu(\Theta = 20^\circ \text{ C})}$$

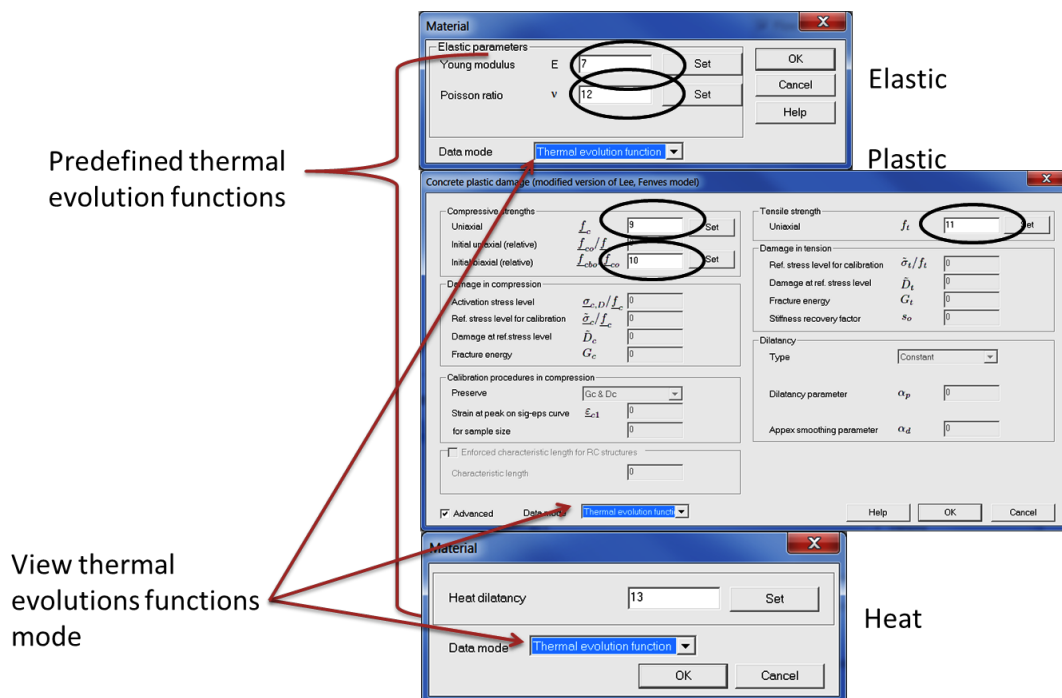
$$k_c(\Theta) = \frac{f_c(\Theta)}{f_c(\Theta = 20^\circ \text{ C})}$$

$$k_{c,D}(\Theta) = \frac{\sigma_{c,D}/f_c(\Theta)}{\sigma_{c,D}/f_c(\Theta = 20^\circ \text{ C})}$$

$$k_{cb}(\Theta) = \frac{f_{cbo}/f_{co}(\Theta)}{f_{cbo}/f_{co}(\Theta = 20^\circ \text{ C})}$$

$$k_{ct}(\Theta) = \frac{f_t(\Theta)}{f_t(\Theta = 20^\circ \text{ C})}$$

In the dialog box for the material data (under standard input mode) user sets reference values of these parameters ie. at assumed temperature $\Theta = 20^\circ \text{ C}$. By switching the input mode to the thermal evolutions functions (see fig.below), once the fire extension is activated, six predefined functions (some of them are based on EC-2) $k_E, k_\nu, k_c, k_{\tilde{D}_c}, k_{cb}, k_{ct}$ are set.

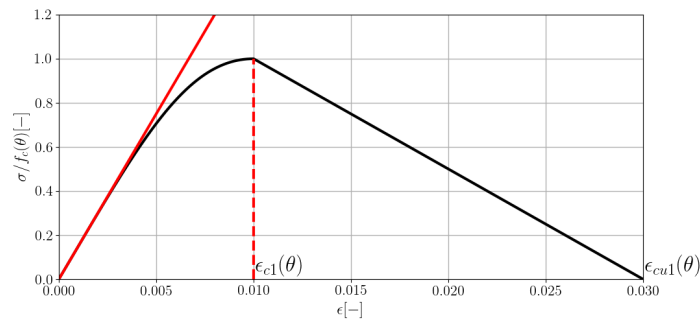


Window 4-2

Window 4-3: EC2 $\sigma - \varepsilon$ relation in compression

ZSoil®

$$\sigma = f_c \frac{3 \left(\frac{\varepsilon}{\varepsilon_{c1}} \right)}{\left(2 + \left(\frac{\varepsilon}{\varepsilon_{c1}} \right)^3 \right)}$$



EC2 $\sigma - \varepsilon$ curve in compression

Remarks:

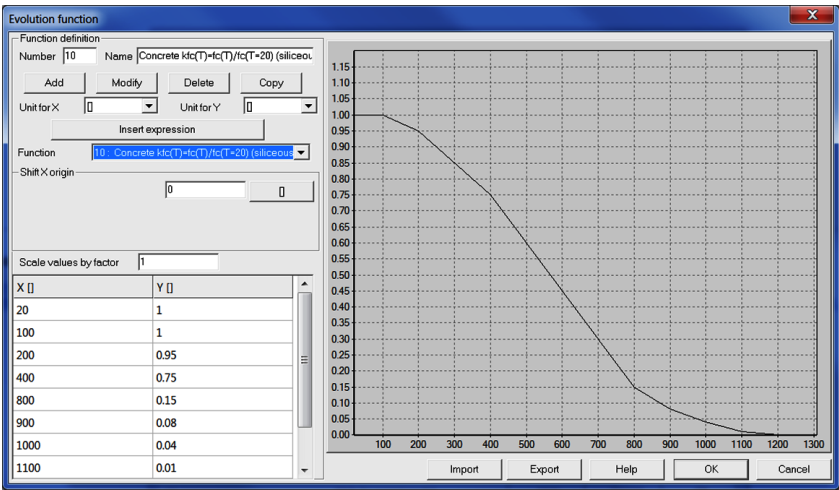
- 1. E modulus is set at $\sigma/f_c \approx 0.4$
- 2. $\frac{\varepsilon}{\varepsilon_{c1}} = 0.26927$ at $\sigma/f_c \approx 0.4$

Window 4-3

Window 4-4: Evolution function $k_c(\Theta)$ for siliceous aggregate

ZSoil®

The $k_c(\Theta)$ function for siliceous aggregate is given in tabular form in the EC2. Its representation is shown in the figure.



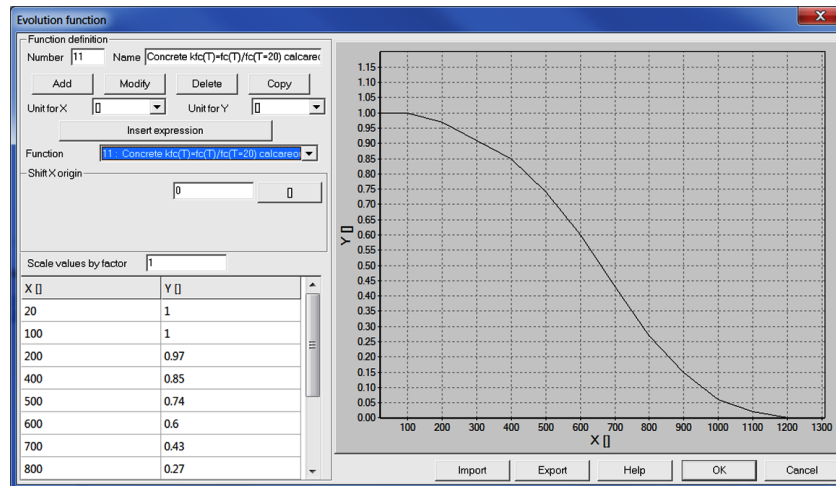
Window 4-4

4.1. THERMAL EVOLUTION FUNCTIONS FOR MECHANICAL PROPERTIES OF CONCRETE

Window 4-5: Evolution function $k_c(\Theta)$ for calcareous aggregate

ZSoil®

The $k_c(\Theta)$ function for calcareous aggregate is given in tabular form in the EC2. Its representation is shown in the figure.



Window 4-5

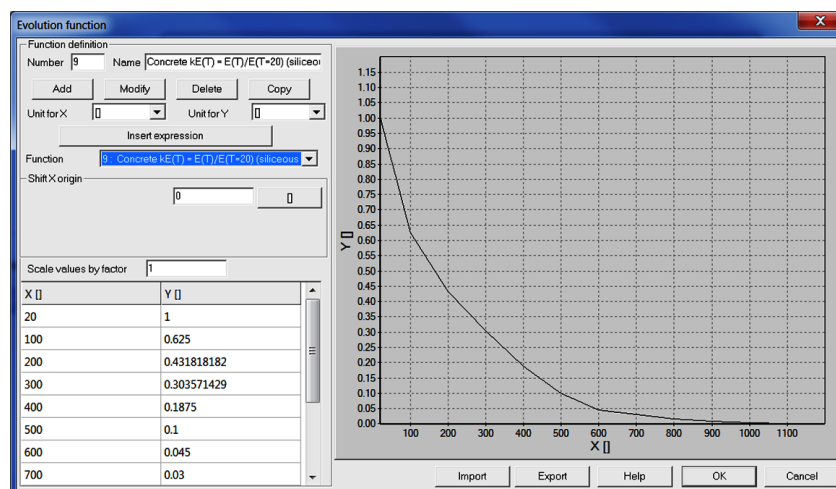
Window 4-6: Evolution function $k_E(\Theta)$ for siliceous aggregate

ZSoil®

The $k_E(\Theta)$ function is not explicitly set in the EC2 standard. However one can derive it from the general definition of the $\sigma - \varepsilon$ curve (see Win.4-3) based on explicit $k_c(\Theta)$ and $\varepsilon_{c1}(\Theta)$ function for the siliceous aggregate.

The $k_E(\Theta)$ function is defined as follows:

$$k_E(\Theta) = \frac{k_c(\Theta)}{\varepsilon_{c1}(\Theta)/\varepsilon_{c1}(\Theta = 20^\circ\text{C})}$$

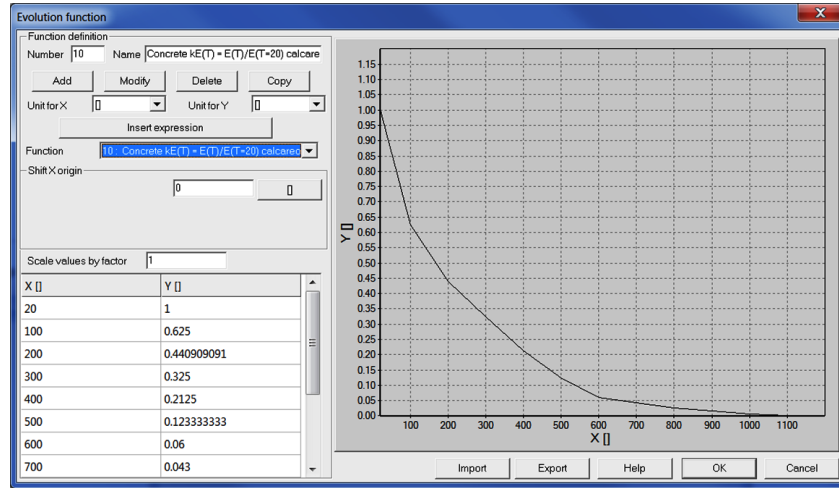


Window 4-6

Window 4-7: Evolution function $k_E(\Theta)$ for calcareous aggregate

ZSoil®

The $k_E(\Theta)$ function is defined as follows (see Win.4-6 for derivation details)



Window 4-7

Window 4-8: Evolution function $k_\nu(\Theta)$

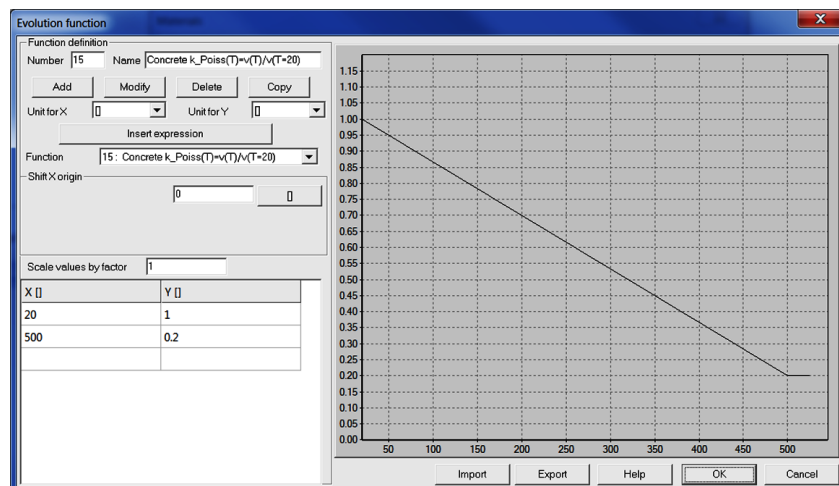
ZSoil®

Thermal dependency of the Poisson's ratio is defined after Marechal (1970)[2].

$$\nu = \begin{cases} \nu_{20} & \text{for } \theta \leq 20^\circ C \\ \nu_{20} \left(0.2 + 0.8 \frac{500 - \theta}{500 - 20} \right) & \text{for } 20^\circ \leq \theta \leq 500^\circ C \\ 0.2 \nu_{20} & \text{for } \theta > 500^\circ C \end{cases}$$

The $k_\nu(\Theta)$ function is defined as follows

$$k_\nu(\Theta) = \frac{\nu(\Theta)}{\nu(\Theta = 20^\circ C)}$$



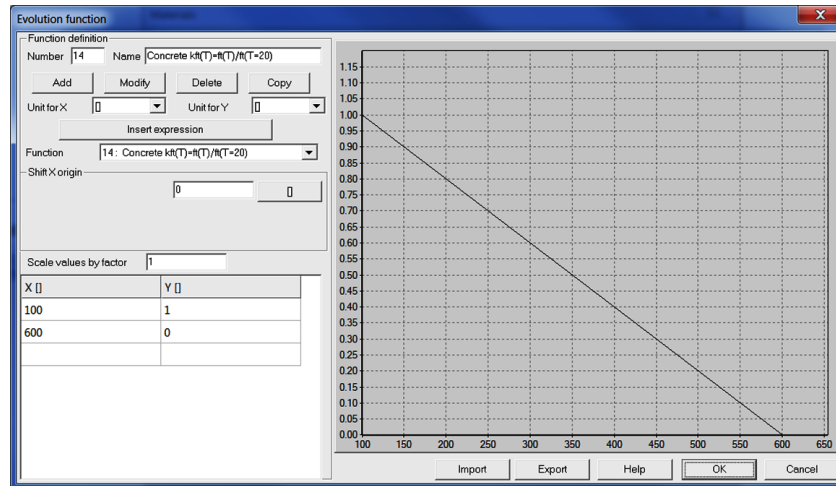
4.1. THERMAL EVOLUTION FUNCTIONS FOR MECHANICAL PROPERTIES OF CONCRETE

Window 4-8

Window 4-9: Evolution function $k_{ct}(\Theta)$

ZSoil®

The $k_{ct}(\Theta)$ function varies linearly from 1.0 at $\Theta = 100^\circ\text{C}$ to 0.0 at $\Theta = 600^\circ\text{C}$ (see EC2), no matter what kind of the aggregate is used. Its representation is shown in the figure.



Window 4-9

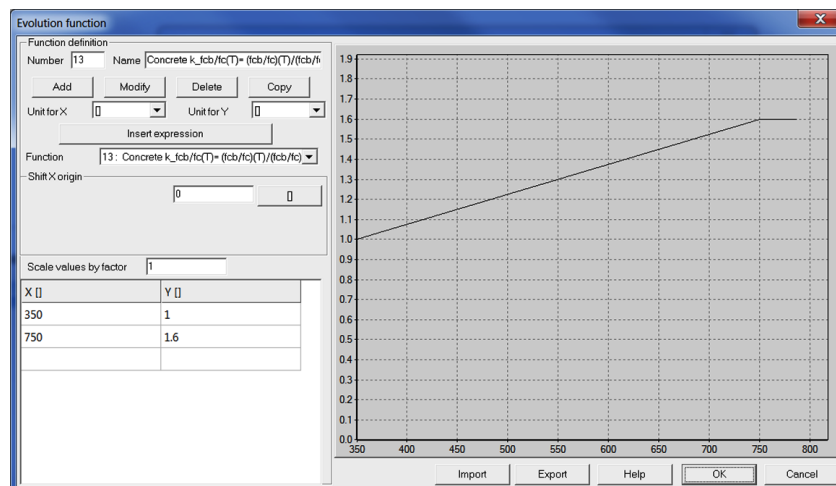
Window 4-10: Evolution function $k_{cb}(\Theta)$

ZSoil®

The $k_{cb}(\Theta)$ function is defined after Gernay [2] (here we assume that the initial and ultimate, biaxial to the uniaxial compressive strength ratios are the same):

$$k_{cb}(\theta) = \begin{cases} f_{cbo}(\theta)/f_{co}(\theta) = 1.16 & \text{for } \Theta < 350^\circ \\ f_{cbo}(\theta)/f_{co}(\theta) = 1.16 (1 + 0.6 \frac{\Theta - 350}{750 - 350}) & \text{for } 350^\circ < \Theta < 750^\circ \end{cases}$$

Its representation is shown in the figure.



Window 4-11: Evolution functions $G_c(\Theta)$ and $f_{co}/f_c(\Theta)$

ZSoil®

In the EC2 standard there is no notion of the G_c parameter. For sake of simplicity we assume that:

$$\frac{G_c(\Theta)}{G_c(\Theta = 20^\circ\text{C})} = k_c(\Theta)$$

$$\frac{f_{co}/f_c(\Theta)}{f_{co}/f_c(\Theta = 20^\circ\text{C})} = \text{const}$$

Remarks:

1. With this hypothesis internal model parameters a_c and b_c remain constant which is crucial to avoid thermodynamically non-admissible states

Window 4-12: Evolution functions for \tilde{D}_c and $\tilde{\sigma}_c/f_c$

ZSoil®

For sake of model simplicity we assume that

$$\tilde{D}_c(\Theta) = \tilde{D}_c(\Theta = 20^\circ\text{C}) \text{ and } \tilde{\sigma}_c/f_c(\Theta) = \tilde{\sigma}_c/f_c(\Theta = 20^\circ\text{C})$$

Remarks:

1. With this hypothesis internal model parameter d_c remains constant which is crucial to avoid thermodynamically non-admissible states
2. Constant value of \tilde{D}_c parameter yields poor match between EC2 model and the current one for temperatures higher than 400°C in the descending branch of $\sigma - \varepsilon$ curve in compression; this drawback can be partially corrected by diminishing \tilde{D}_c value for temperatures higher than 400°C ; therefore user may set his own evolution function understood as $k_{\tilde{D}_c} = \frac{\tilde{D}_c(\Theta)}{\tilde{D}_c(\Theta = 20^\circ\text{C})}$; this evolution function must be defined with care because too low value of \tilde{D}_c parameter may lead to violation of the condition put on internal model parameters $d_c \geq b_c$ (see report on plastic damage model); in such cases $\sigma_{c,D}/f_c$ value will artificially be enlarged in the calculation module during the analysis; this correction, however, may preclude degradation of $\sigma_{c,D}/f_c$ till its minimal value that is equal to $(\sigma_{c,D}/f_c)_{\min} = f_{co}/f_c$

Window 4-13: Evolution function for $G_t(\Theta)$

ZSoil®

4.1. THERMAL EVOLUTION FUNCTIONS FOR MECHANICAL PROPERTIES OF CONCRETE

For sake of simplicity we assume that:

$$\frac{G_t(\Theta)}{G_t(\Theta = 20^\circ\text{C})} = k_{ct}(\Theta)$$

Remarks:

1. With this hypothesis internal model parameters a_t and b_t remain constant which is crucial to avoid thermodynamically non-admissible states

Window 4-13

Window 4-14: Evolution functions for \tilde{D}_t and $\tilde{\sigma}_t/f_t$

ZSoil®

For sake of model simplicity we assume that

$$\tilde{D}_t(\Theta) = \tilde{D}_t(\Theta = 20^\circ\text{C}) \text{ and } \tilde{\sigma}_t/f_t(\Theta) = \tilde{\sigma}_t/f_t(\Theta = 20^\circ\text{C})$$

Remarks:

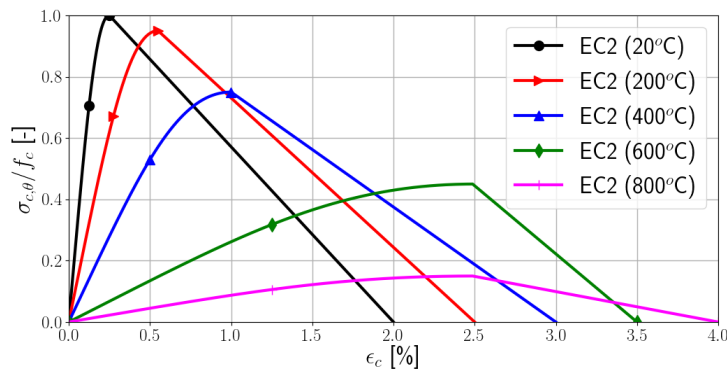
1. With this hypothesis internal model parameter d_t remains constant which is crucial to avoid thermodynamically non-admissible states

Window 4-14

Window 4-15: Evolution function for $k_{c,D}$

ZSoil®

In the EC2 the recommended shape of $\sigma - \epsilon$ curves in uniaxial compression test is shown in the figure.



CHAPTER 4. EXTENSION OF THE PLASTIC DAMAGE MODEL TO HANDLE FIRE PROBLEMS

It is well visible that descending branches become shorter with increasing temperature. This effect cannot be reproduced with the model but discrepancies can be reduced by degrading stress level at which damage starts to occur. In the modified version of the model damage can be delayed with respect to the onset of plastic straining. Hence we assume that:

$$\frac{\sigma_{c,D}}{f_c}(\Theta) = \begin{cases} \frac{\sigma_{c,D}}{f_c}(\Theta = 20^\circ\text{C}) & \text{for } \Theta \leq 200^\circ\text{C} \\ \frac{\sigma_{c,D}}{f_c}(\Theta = 20^\circ\text{C}) \frac{600 - \Theta}{200} + \frac{\sigma_{co}}{f_c}(\Theta = 20^\circ\text{C}) \frac{\Theta - 200}{400} & \text{for } 200^\circ \leq \Theta \leq 600^\circ\text{C} \\ \frac{\sigma_{co}}{f_c}(\Theta = 20^\circ\text{C}) & \text{for } \Theta > 400^\circ\text{C} \end{cases}$$

NB. The resulting evolution function $k_{c,D}$ is not shown in the user interface.

Remarks:

1. The above evolution function can be internally modified due to condition $d_c \geq b_c$ that must always be satisfied (see report on plastic damage model); in all limiting cases $\sigma_{c,D}/f_c$ value is internally corrected by the calculation module during the analysis

Window 4-15

4.2 Transient creep

Window 4-16: Strain decomposition

ZSoil®

Effective strain that generates stresses can be decomposed as follows:

$$\Delta\varepsilon^{eff} = \Delta\varepsilon - \Delta\varepsilon^o - \Delta\varepsilon^{cr,tr} - \Delta\varepsilon^{cr,std}$$

where:

$\Delta\varepsilon$ - increment of total strains

$\Delta\varepsilon^o = \alpha_c(\Theta) \Delta\Theta$ - increment of thermal strains

$\Delta\varepsilon^{cr,std}$ - increment of standard creep strains

$\Delta\varepsilon^{cr,tr}$ - increment of transient creep strains

Remarks:

1. Under fire conditions standard creep strains $\Delta\varepsilon^{cr,std}$ are relatively small due to short time regime; therefore these strains are neglected in further model development
2. Transient creep strains $\Delta\varepsilon^{cr,tr}$ are significant; these strains are caused by temperature variation
3. Transient creep strains are produced in the effective configuration (in damage sense) and not nominal one

Window 4-16

Window 4-17: Explicit transient creep

ZSoil®

Increment of transient creep strains is computed following the idea proposed by Gernay [2]:

$$\Delta \varepsilon_{N+1}^{cr, tr} = (\Phi(\Theta_{N+1}) - \Phi(\Theta_N)) \mathbf{D}_o^{-1} \frac{1}{f_c(20^\circ\text{C})} \bar{\sigma}_N^-$$

where:

$\Phi(\Theta_{N+1})$ - is the transient creep function given in the tabular form depending on the aggregate type

$\bar{\sigma}_N^-$ - negative part of the effective stress tensor

\mathbf{D}_o^{-1} - dimensionless projection matrix (equivalent here to the elastic compliance matrix computed for unit E modulus)

According to Gernay [2] transient creep strains are produced if the following three conditions are satisfied

- At least one principal stress is compressive
- Stress state is in the pre-peak branch of $\sigma - \varepsilon$ curve (in compression; $\kappa_c \leq \kappa_{c, peak}$)
- Current temperature is higher than the maximum registered one during stage of heating

Remarks:

1. The negative part of the stress tensor is computed in the following manner
 - For given effective stress state $\bar{\sigma}_N^-$ three principal stresses $\bar{\sigma}_i$ and three eigenbases \mathbf{m}_i are computed
 - $\bar{\sigma}_N^- = \sum_{i=1}^3 H(-\bar{\sigma}_i) \bar{\sigma}_i \mathbf{m}_i$
2. According to Anderberg et al.[3] transient creep strains are proportional to thermal strains ($\varepsilon^{cr, tr} \approx k_2 \frac{\sigma}{f_c(\Theta = 20^\circ\text{C})} \varepsilon^o(\Theta)$); in damage model creep is present at the effective stress configuration, therefore the creep function $\Phi(\Theta)$ can be set as: $\Phi(\Theta) = k_2 \varepsilon^o(\Theta)$ ($k_2 \approx 2.35$ after Anderberg et al.); to generalize the approach we propose to modify creep law to the following form

$$\Delta \varepsilon_{N+1}^{cr, tr} = \Phi_{ref} (\Phi(\Theta_{N+1}) - \Phi(\Theta_N)) \mathbf{D}_o^{-1} \frac{1}{f_c(20^\circ\text{C})} \bar{\sigma}_N^-$$
 where creep function $\Phi(\Theta) \approx \varepsilon^o(\Theta)$ while $\Phi_{ref} = k_2$ (after Anderberg et al.);

Window 4-17

Chapter 5

Benchmarks

5.1 Truss element in displacement driven tensile test at elevated temperatures

Comparison of the EC2 model for the steel reinforcement and numerical predictions of the $\sigma - \varepsilon$ curves in the uniaxial tensile tests is the aim of this benchmark. In the first stage thermal analysis is carried out with aid of a single Q4 element in which constant temperature is imposed at all nodes. In the second stage single 2-node truss element (of unit length) is subject to tension using displacement driven loading program and temperature field taken from thermal analysis. The test setup is shown in the following figure. Imposed displacement is applied at node 2 of the truss element.

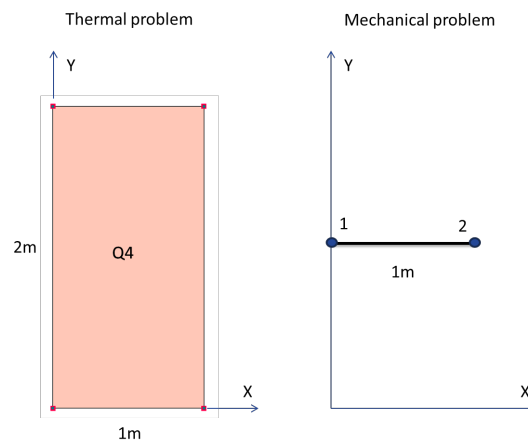


Figure 5.1: Truss element subject to displacement driven loading program at constant elevated temperature

5.1.1 Thermal analysis

Files for thermal analysis:

Fire-Q4-thermal-100C.inp, Fire-Q4-thermal-400C.inp, Fire-Q4-thermal-700C.inp

Generating constant temperature field that can be associated with the truss element is the aim of thermal analysis. As truss elements cannot be used in heat transfer analysis a single Q4 element is used instead and temperatures at all its nodes are fixed to a given assumed value. As the temperature is constant thermal strains are zero and assumed thermal properties of a material associated with the Q4 element are not meaningful. In this test the following set of thermal properties is used

Parameter	Unit	Value
λ_c	[MW/mK]	$1.9514 \cdot 10^{-6}$
c_c^*	[MJ/m ³ K]	2.160
α_c	[1/K]	$9.128 \cdot 10^{-6}$

5.1.2 Mechanical analysis

Files for mechanical analysis:

Fire-Q4-truss-elongation-100C.inp, Fire-Q4-truss-elongation-400C.inp,

Fire-Q4-truss-elongation-700C.inp,

Fire-Q4-truss-elongation-400C-cyclic.inp, Fire-Q4-truss-elongation-700C-cyclic.inp

In the mechanical part of this benchmark a single two node truss element 1m long (with unit cross section area $A = 1\text{m}^2$) is elongated using displacement driven loading program while its mechanical properties depend on the temperature (obtained from thermal project). As the temperature is constant no thermal strains are produced. To check model behavior both monotonic and cyclic tests were carried out.

Material properties of a steel bar are summarized in the following table.

Parameter	Unit	Value
E	[MPa]	200000
f_c	[MPa]	500.0
f_t	[MPa]	500.0
α_s	[1/K]	$1.216 \cdot 10^{-5}$

Comparizon of the current model and the EC2 one response in the monotonic uniaxial tensile test for three different elevated temperatures 100°C, 400°C, 700°C is shown in the following figure. Results of cyclic tests in double way cyclic test is shown in the next figure.

5.1. TRUSS ELEMENT IN DISPLACEMENT DRIVEN TENSILE TEST AT ELEVATED TEMPERATURES

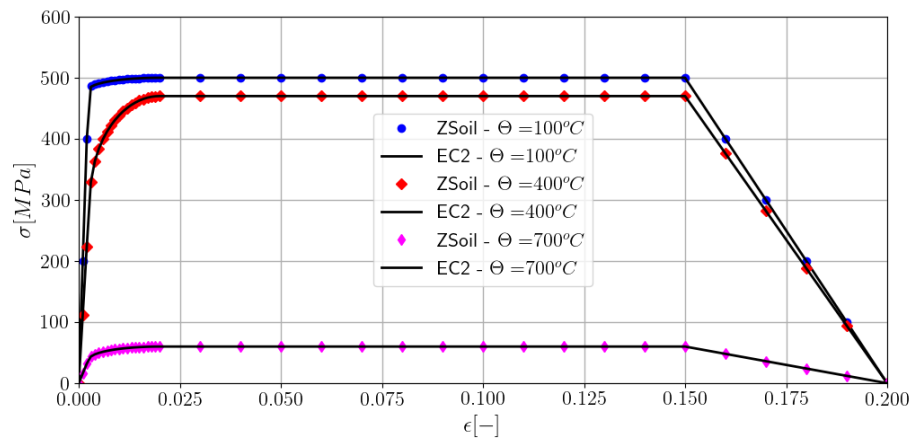


Figure 5.2: Stress-strain curves for $\Theta = 100^\circ\text{C}$, $\Theta = 400^\circ\text{C}$, $\Theta = 700^\circ\text{C}$ in monotonic tensile test

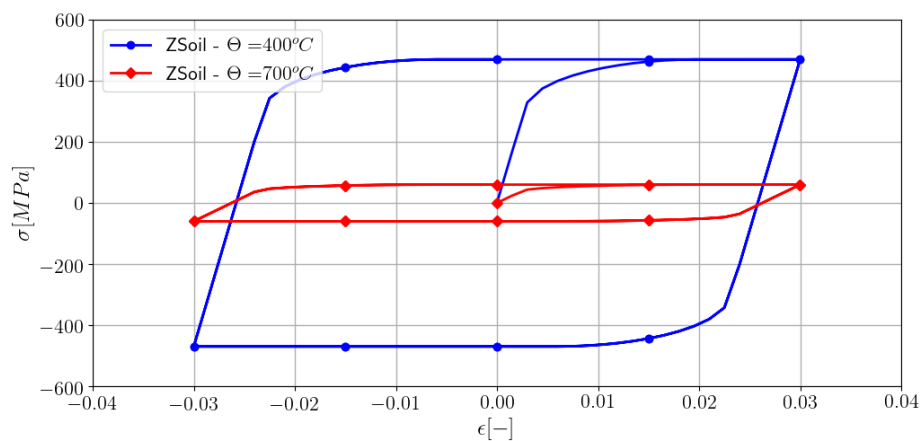


Figure 5.3: Stress-strain curves for $\Theta = 400^\circ\text{C}$, $\Theta = 700^\circ\text{C}$ in cyclic test

5.2 Displacement driven uniaxial compression test of plain concrete at elevated temperatures

Comparison of the EC2 model and numerical predictions of the $\sigma - \varepsilon$ curves for concrete (siliceous aggregate), in the uniaxial compression test, is the aim of this benchmark. In the first stage thermal analysis is carried out with aid of a single Q4 element in which constant temperature is imposed at all nodes. In the second stage single Q4 axisymmetric element (of the same size) is subject to compression using displacement driven loading program and temperature field taken from thermal analysis. The test setup is shown in the following figure. Imposed vertical displacements are applied at nodes 2 and 3.

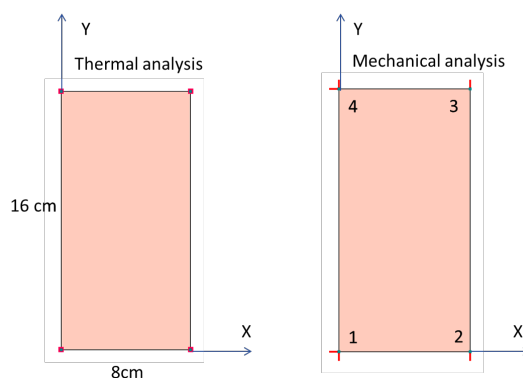


Figure 5.4: Q4 axisymmetric element subject to uniaxial compression (displacement driven loading program) at constant elevated temperatures

5.2.1 Thermal analysis

Files for thermal analysis:

Fire_CDPM_1D_comp_T_20_heat_prj.inp,
Fire_CDPM_1D_comp_T_200_heat_prj.inp,
Fire_CDPM_1D_comp_T_400_heat_prj.inp,
Fire_CDPM_1D_comp_T_600_heat_prj.inp,
Fire_CDPM_1D_comp_T_800_heat_prj.inp

Generating constant temperature field that can later be associated with the continuum element subject to the uniaxial compression is the aim of carried out thermal analysis. As the temperature is constant thermal strains are zero and assumed thermal properties of a material associated with the Q4 element are not meaningful. In this test the following set of thermal properties is used

Parameter	Unit	Value
λ_c	[MW/mK]	$1.9514 \cdot 10^{-6}$
c_c^*	[MJ/m ³ K]	2.160
α_c	[1/K]	$9.128 \cdot 10^{-6}$

5.2.2 Mechanical analysis

Files for mechanical analysis:

Fire_CDPM_1D_comp_T_20.inp,
Fire_CDPM_1D_comp_T_200.inp,
Fire_CDPM_1D_comp_T_400.inp,
Fire_CDPM_1D_comp_T_600.inp,
Fire_CDPM_1D_comp_T_800.inp,
Fire_CDPM_1D_comp_T_600_Dc_var.inp,
Fire_CDPM_1D_comp_T_800_Dc_var.inp

In the mechanical part of this benchmark a single axisymmetric Q4 element (8cm x 16 cm) (radius is equal to 8cm !) is compressed using displacement driven loading program while its mechanical properties depend on the temperature (obtained from thermal project). As the temperature is constant no thermal neither transient creep strains are produced. In order to achieve reasonable match of the model response with respect to the EC2 one value of the $\underline{\sigma}_{c,D}/\underline{f}_c$ parameter must be larger than the $\underline{f}_{co}/\underline{f}_c$. Material properties are summarized in the following table.

Parameter	Unit	Value
E	[MPa]	27000
ν	[-]	0.20
\underline{f}_c	[MPa]	38.0
$\underline{f}_{co}/\underline{f}_c$	[-]	0.4
$\underline{f}_{cbo}/\underline{f}_{co}$	[-]	1.16
$\underline{\sigma}_{c,D}/\underline{f}_c$	[-]	0.75

$\tilde{\sigma}_c/f_c$	[-]	1.0
\tilde{D}_c	[-]	0.435
G_c	[MN/m]	$5 \cdot 10^{-3}$
f_t	[MPa]	2.9
$\tilde{\sigma}_t/f_t$	[-]	0.5
\tilde{D}_t	[-]	0.5
G_t	[MN/m]	10^{-4}
s	[-]	0.2
Dilatancy		Constant
α_p	[-]	0.2
α_d	[-]	1.0

Comparison of the EC2 and ZSoil model responses for $\Theta = 20^\circ\text{C}$, $\Theta = 200^\circ\text{C}$, $\Theta = 400^\circ\text{C}$, $\Theta = 600^\circ\text{C}$, $\Theta = 800^\circ\text{C}$ is shown in the following figures.

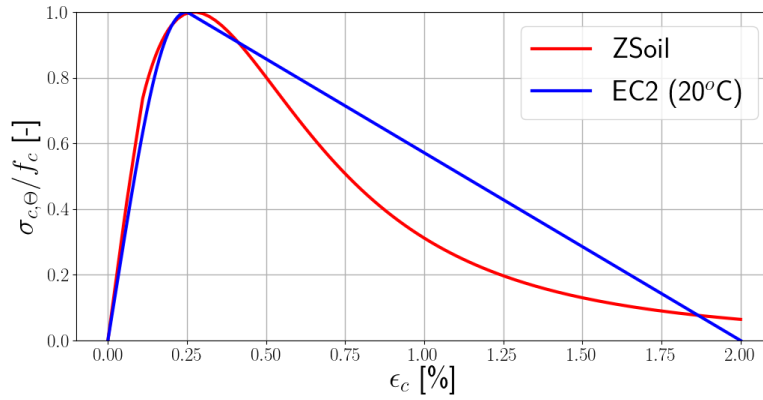


Figure 5.5: $\sigma - \varepsilon$ curves for $\Theta = 20^\circ\text{C}$ (constant \tilde{D}_c)

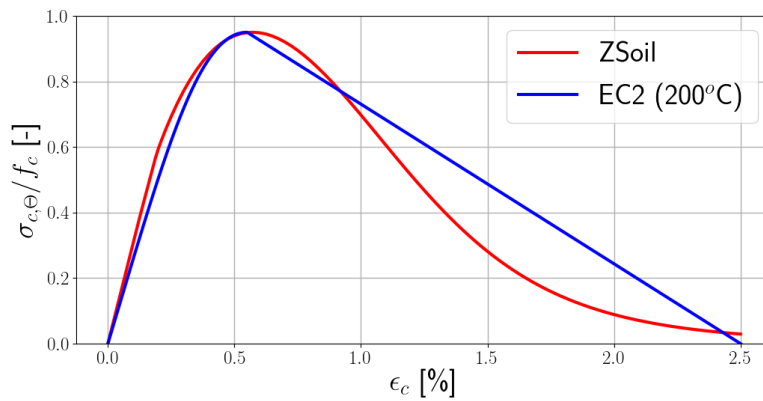


Figure 5.6: $\sigma - \varepsilon$ curves for $\Theta = 200^\circ\text{C}$ (constant \tilde{D}_c)

5.2. DISPLACEMENT DRIVEN UNIAXIAL COMPRESSION TEST OF PLAIN CONCRETE AT ELEVATED TEMPERATURES

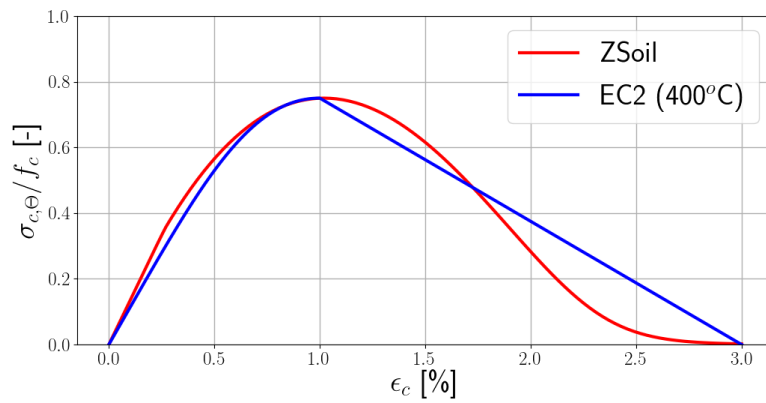


Figure 5.7: $\sigma - \varepsilon$ curves for $\Theta = 400^\circ\text{C}$ (constant \tilde{D}_c)

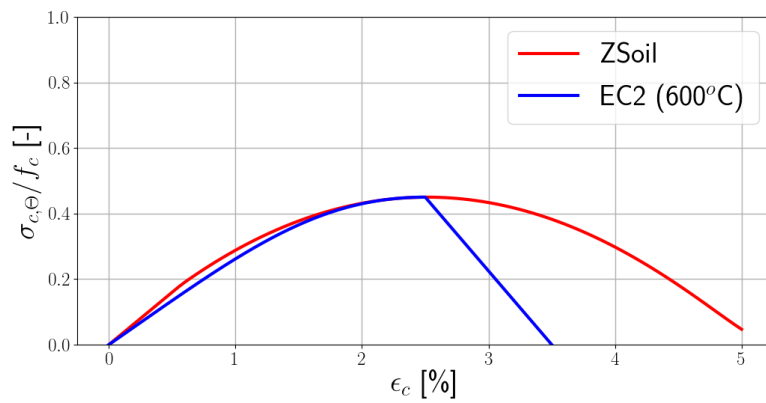


Figure 5.8: $\sigma - \varepsilon$ curves for $\Theta = 600^\circ\text{C}$ (constant \tilde{D}_c)

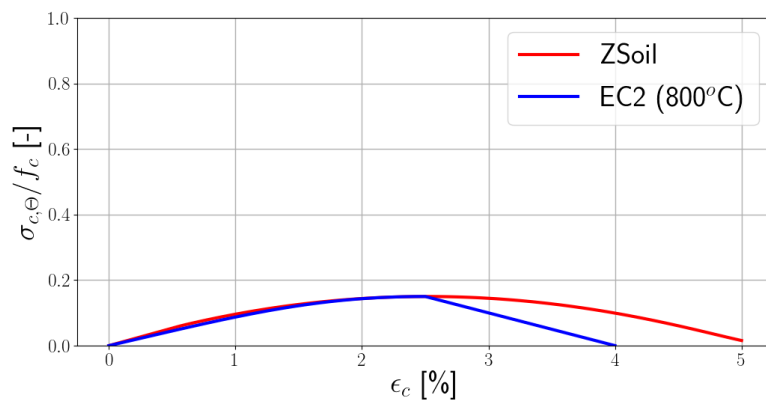


Figure 5.9: $\sigma - \varepsilon$ curves for $\Theta = 800^\circ\text{C}$ (constant \tilde{D}_c)

It is well visible that the EC2 model and the current one deviate in the post peak branch for temperatures higher than 400°C . To obtain better match it is possible to define an evolution function for the \tilde{D}_c parameter (user can define his own function, although it has to be done with care). Here we assume that till $\Theta = 400^{\circ}\text{C}$ \tilde{D}_c remains constant and equal to $\tilde{D}_c = 0.435$. Then it drops down to value $\tilde{D}_c = 0.41$ at $\Theta = 600^{\circ}\text{C}$. The resulting $\sigma - \varepsilon$ curves for $\Theta = 600^{\circ}\text{C}$ and $\Theta = 800^{\circ}\text{C}$ are shown in next two figures. This modification slightly improves resulting stress-strain curves.

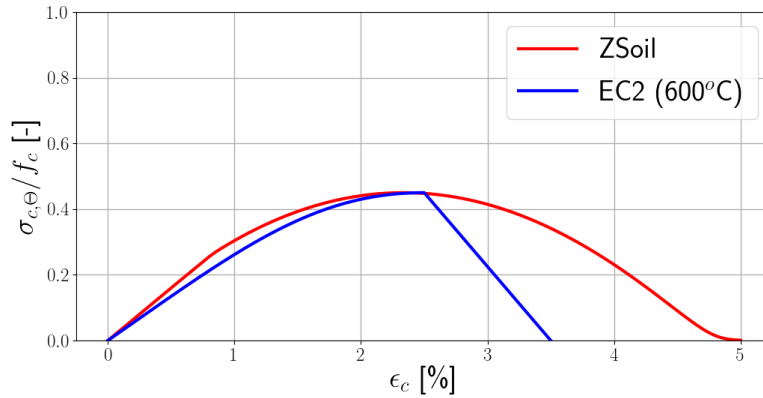


Figure 5.10: $\sigma - \varepsilon$ curves for $\Theta = 600^{\circ}\text{C}$ (variable \tilde{D}_c)

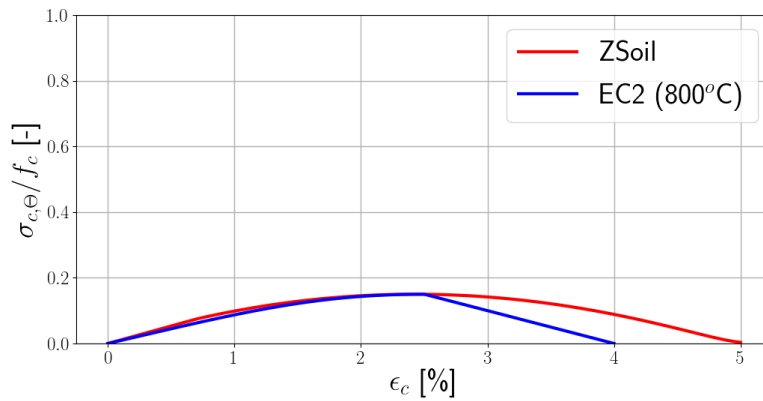


Figure 5.11: $\sigma - \varepsilon$ curves for $\Theta = 800^{\circ}\text{C}$ (variable \tilde{D}_c)

5.3 Anderberg and Thelandersson test

Comparison of the test results of experiment (sample A, tests A6, A7, A8, A9), carried out by Anderberg and Thelandersson [?], and numerical predictions carried out with aid of the modified Lee-Fenves model is the aim of this benchmark. In the considered tests concrete cylindrical samples (radius 7.5cm and height 15cm) were preloaded, at temperature $\Theta = 25^{\circ}\text{C}$, to the assumed percentage of the nominal compression strength (in the test A6 it was 0.225, in A7 0.35, in A8 0.45 and in A9 0.675), and then heated with the constant rate $5^{\circ}\text{C}/\text{min}$ until failure. As the transient creep is driven by the temperature increase and the stress state, real rate dependency is not present. The EC2 thermal evolution functions are not fully coherent with the measurements in the real laboratory test therefore the EC2 model parameters and evolution functions are used here. The resulting sample deformations can still be compared with the test results due to similarity of evolution of thermal and transient creep strains. To model these tests thermal analysis is carried out first using single Q4 axisymmetric element in which all temperatures are constrained by the temperature boundary condition. In the second stage mechanical analysis is run using thermal field generated in the first stage. The test setup is shown in the following figure.

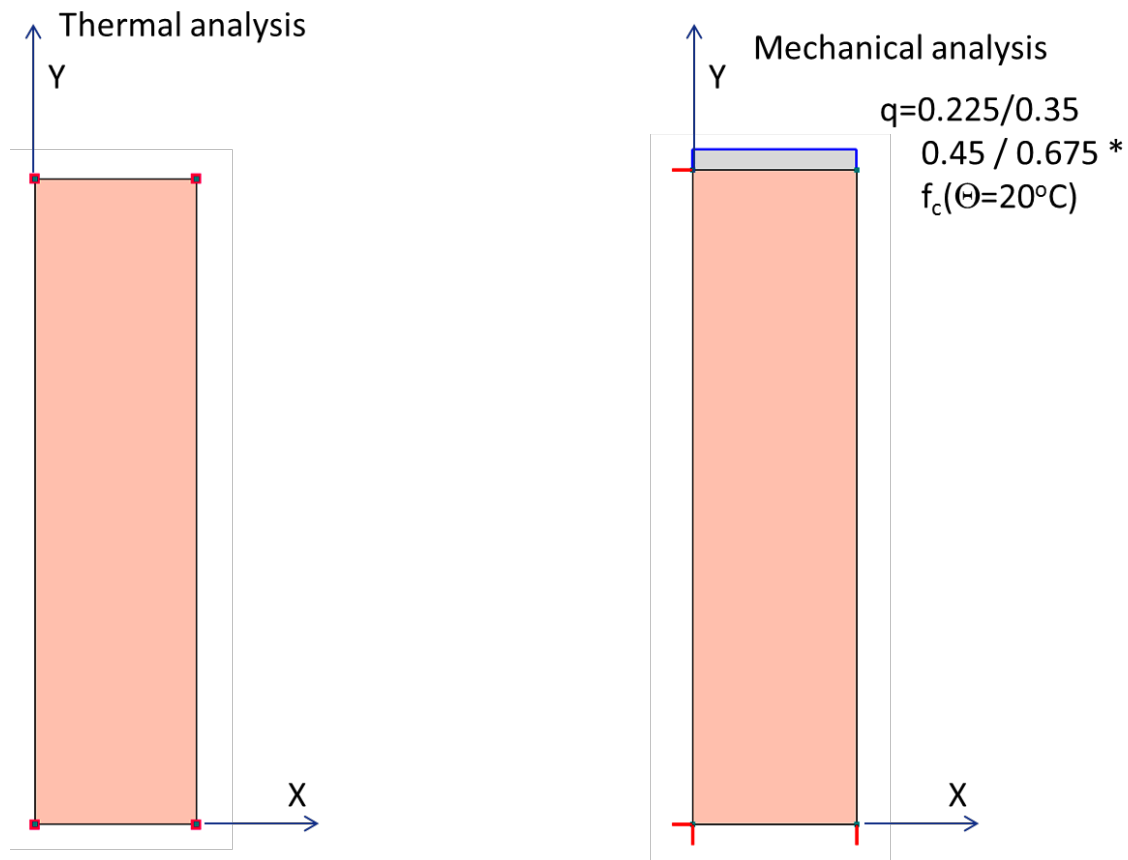


Figure 5.12: Q4 axisymmetric element subject to progressive heating (preloading is executed first)

5.3.1 Thermal analysis

Files for thermal analysis:

Fire_Anderberg_A_heat_prj.inp

Generating variable (in time) temperature field, that can later be associated with the continuum element, subject to the uniaxial compression, is the aim of carried out thermal analysis. In this test the following set of thermal properties is used (siliceous aggregate)

Parameter	Unit	Value
λ_c	[MN/min K]	$1.17084 \cdot 10^{-4}$
c_c^*	[MJ/m ³ K]	2.160
α_c	[1/K]	$9.128 \cdot 10^{-6}$

5.3.2 Mechanical analysis

Files for mechanical analysis:

Fire_Anderberg_A_0_225.inp,

Fire_Anderberg_A_0_35.inp,

Fire_Anderberg_A_0_45.inp ,

Fire_Anderberg_A_0_675.inp

In the mechanical part of this benchmark a single axisymmetric Q4 element (3.75cm x 15 cm) (radius is equal to 3.75 cm !) is initially compressed (at temperature 25°C) until assumed percentage of the uniaxial compressive strength and then subject to progressive heating with a constant rate 5°C/min. **Evolution functions designed for the siliceous aggregate are selected here.** Material properties are summarized in the following table.

Parameter	Unit	Value
E	[MPa]	27000
ν	[-]	0.20
\underline{f}_c	[MPa]	38.0
$\underline{f}_{co}/\underline{f}_c$	[-]	0.4
$\underline{f}_{cho}/\underline{f}_{co}$	[-]	1.16
$\underline{\sigma}_{c,D}/\underline{f}_c$	[-]	0.75
$\underline{\tilde{\sigma}}_c/\underline{f}_c$	[-]	1.0
\underline{D}_c	[-]	0.435
G_c	[MN/m]	$5 \cdot 10^{-3}$
f_t	[MPa]	2.9
$\tilde{\sigma}_t/f_t$	[-]	0.5
\underline{D}_t	[-]	0.5
G_t	[MN/m]	10^{-4}
s	[-]	0.2
Dilatancy		Constant
α_p	[-]	0.2
α_d	[-]	1.0

Φ_{ref}	[-]	2.35
--------------	-----	------

To compare Anderberg et al. test results and ZSoil prediction vertical strain time history is analyzed (time on the horizontal axis is replaced by the temperature). One may notice some discrepancies between prediction and experiment for stress level values 0.225 and 0.675. The major reason is such that the EC2 degradation function $k_c(\Theta)$ does not match the result of Anderberg's test. This is especially visible in the test carried out at highest stress ratio ie. 0.675. However this kind of agreement has to be evaluated as good. It is better than the one shown in the paper by Gernay et al.[2].

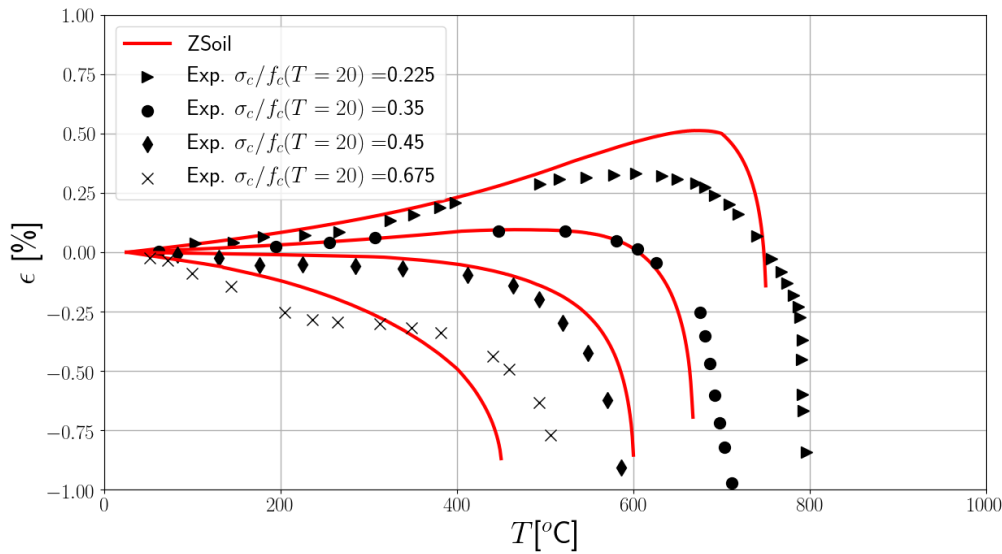


Figure 5.13: Evolution of vertical strain during heating for tests A6, A7, A8, A9

5.4 Slab subject to fire conditions (Lim and Wade test)

Comparizon of the Lim and Wade [4] test results, for the slab HD12 subject to fire conditions, and numerical predictions using modified Lee-Fenves model is the aim of this benchmark. In this test a simply supported rectangular slab 4.3m x 3.3m (taking into account width of the supporting frame profiles nominal slab dimensions are 4.02m x 3.02m), 100mm thick, reinforced in two directions $\phi 12\text{mm}/200\text{mm}$ (hot rolled deformed bars), is initially loaded by the dead weight (24kN/m^3) and live load 3.0kN/m^2 and then subject to the fire conditions applied to the bottom face. Concrete cover is 25mm for the reinforcement set placed along shorter edge and 38mm for the one along longer edge.

This benchmark cannot be solved in a highly accurate manner as during the test corner zones of the slab were uplifting so it was impossible to keep uniform thermal conditions under the slab. Here we assume that these conditions are uniform in thermal stage of the analysis. Thermal part of this benchmark is solved with aid of B8 continuum elements together with convection and radiation boundary conditions. In the mechanical part layered Q4 shell elements are used. The test setup is shown in the following figure.

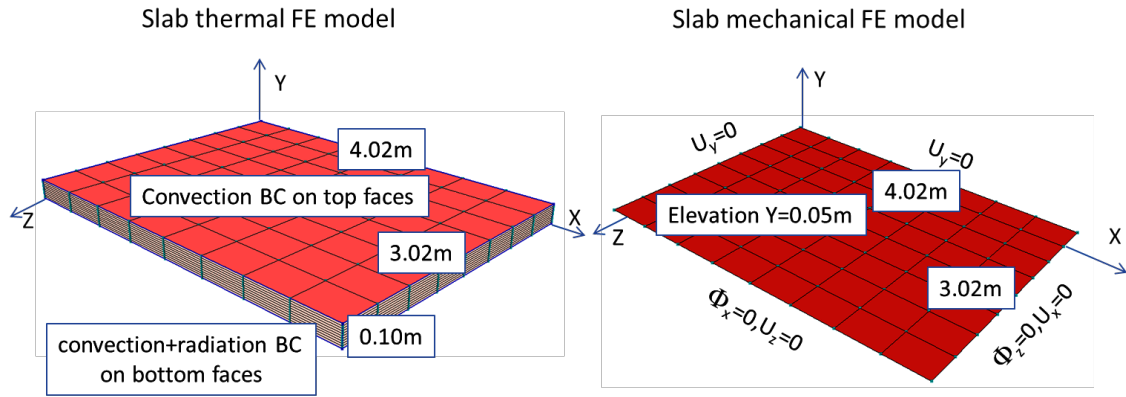


Figure 5.14: Slab subject to the fire conditions (thermal and mechanical setups)

5.4.1 Thermal analysis

Files for thermal analysis:
Fire_Lim_Wade_heat_prj.inp

Generating variable (in time) temperature field, that can later be associated with the slab is the aim of carried out thermal analysis. In this project domain is discretized with $8 \times 8 \times 10$ B8 continuum elements (10 elements across the thickness) while steel reinforcement is neglected (here we assume that steel bars have same temperature as concrete). On top of the mesh convection elements are put assuming that the ambient temperature is constant and equal to 10°C . On the bottom boundary of the mesh both convection and radiation elements are put with the ambient temperature driven by the modified ISO 834 fire curve (here the initial temperature is 10° instead of 20°) ($\Theta(t) = 10 + 345 \log_{10}(8t + 1)$ (time in [min])) In this test the following set of thermal properties is used (siliceous aggregate)

Parameter	Unit	Value
λ_c	[MN/min K]	$1.17084 \cdot 10^{-4}$
c_c^*	[MJ/m ³ K]	2.160
α_c	[1/K]	$9.128 \cdot 10^{-6}$
h_c	[MN/m/min/K]	$1.5 \cdot 10^{-3}$
ϕ	[-]	1.0
ε_m	[-]	0.8
ε_f	[-]	1.0
σ	[MN/ m ³ min K ⁴]	$3.402 \cdot 10^{-12}$

Remarks:

1. Convection coefficient h_c corresponds to the EC2 recommended value $25 \text{ W/m}^2\text{K}$

Maximum and averaged temperature on unheated surface is shown in the following figure. Temperature time history at lower reinforcement location is shown in the next figure. Very good agreement is observed as far as the second result is concerned.

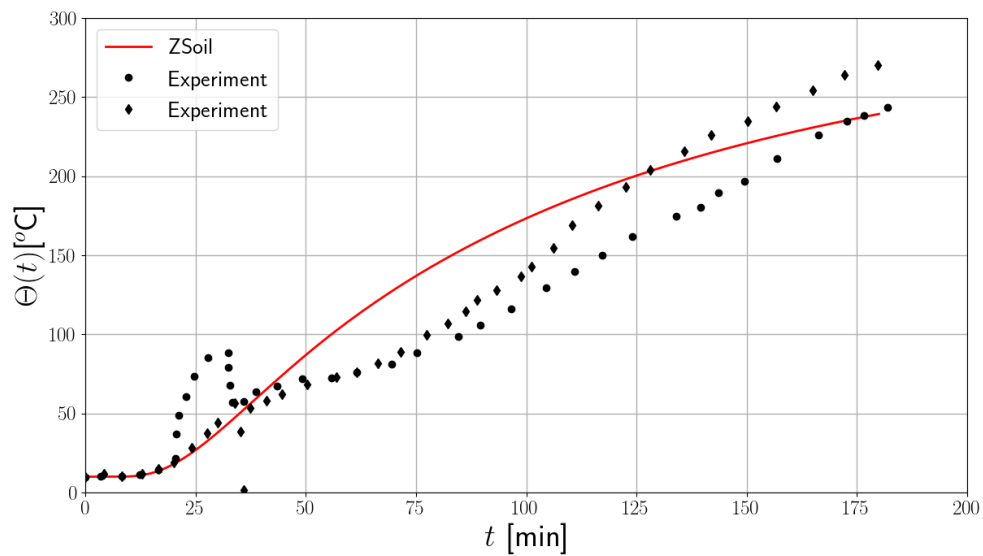


Figure 5.15: Temperature time history on top slab surface

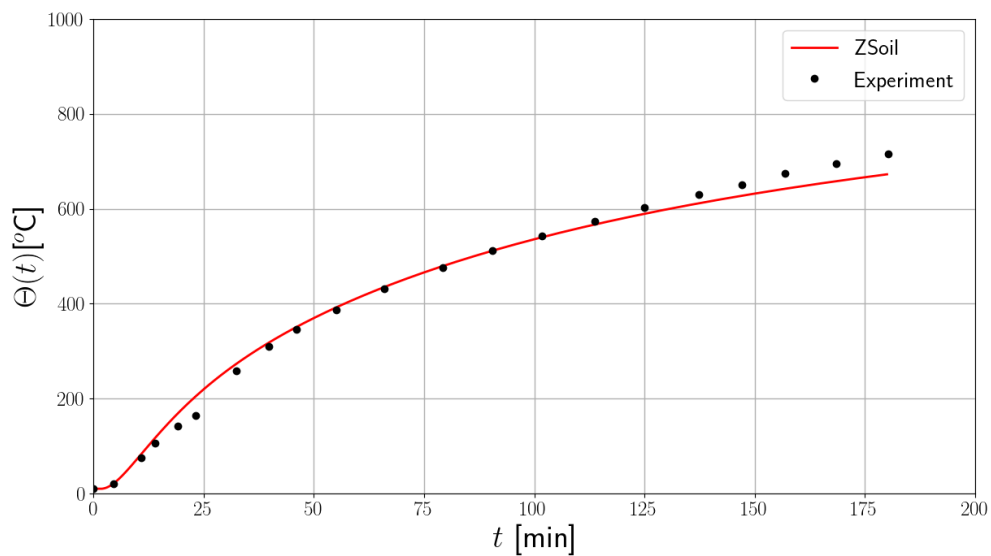


Figure 5.16: Temperature time history in reinforcement bars

5.4.2 Mechanical analysis

Files for mechanical analysis:

Fire_Lim_Wade_mech_prj_A.inp,

Fire_Lim_Wade_mech_prj_B.inp

In the mechanical part of this benchmark domain is discretized with aid of layered Q4 shell elements. By default 10 equal size core material layers are generated in the shell cross

section plus two layers of fiber type steel reinforcement ($565\text{mm}^2/\text{m}$) (hot rolled deformed bars). **Evolution functions designed for the siliceous aggregate are selected here.** Material properties of concrete are summarized in the following table.

Parameter	Unit	Value
E	[MPa]	27000
ν	[-]	0.20
f_c	[MPa]	36.7
$\underline{f}_{co}/\underline{f}_c$	[-]	0.4
$\underline{f}_{cho}/\underline{f}_{co}$	[-]	1.16
$\underline{\sigma}_{c,D}/\underline{f}_c$	[-]	0.75
$\underline{\tilde{\sigma}}_c/\underline{f}_c$	[-]	1.0
\underline{D}_c	[-]	0.435
G_c	[MN/m]	$5 \cdot 10^{-3}$
f_t	[MPa]	2.9
$\underline{\tilde{\sigma}}_t/f_t$	[-]	0.5
\underline{D}_t	[-]	0.5
G_t	[MN/m]	10^{-4}
s	[-]	0.2
Dilatancy		Constant
α_p	[-]	0.2
α_d	[-]	1.0
Φ_{ref}	[-]	2.35

As the structure is reinforced fracture energy is not scaled by the finite element size but by an assumed characteristic length $l_c^{RC} = 0.05\text{m}$.

Material properties for steel reinforcement are summarized in the next table (two different values of steel strength are used).

Parameter	Unit	Value
E	[MPa]	200000
f_t	[MPa]	470(A)/500(B)
f_c	[MPa]	470(A)/500(B)

Central deflection time histories computed and measured are shown in next two figures for two different values of steel strength at ambient conditions. As we can see deflection is underestimated at the beginning of the test while overestimated at the end of the test. The main reason is such that except concrete compressive strength and steel strength no other data is given, hence all other parameters are based on EC2 recommendations. Moreover measurements of temperatures indicate relatively high scatter between different slab zones. In the qualitative sense results are correct.

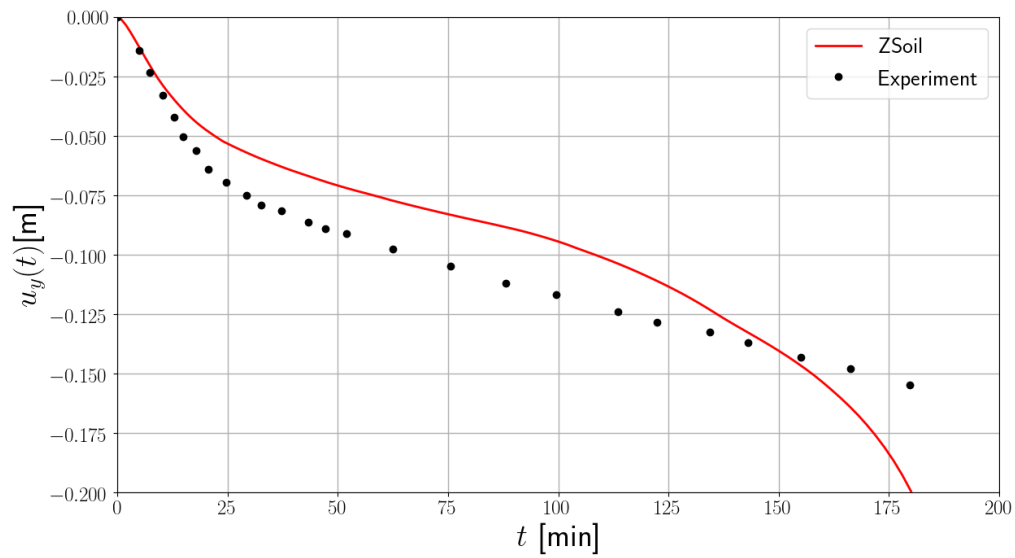


Figure 5.17: Central point deflection time history (steel strength $f_t = f_c = 470$ MPa)

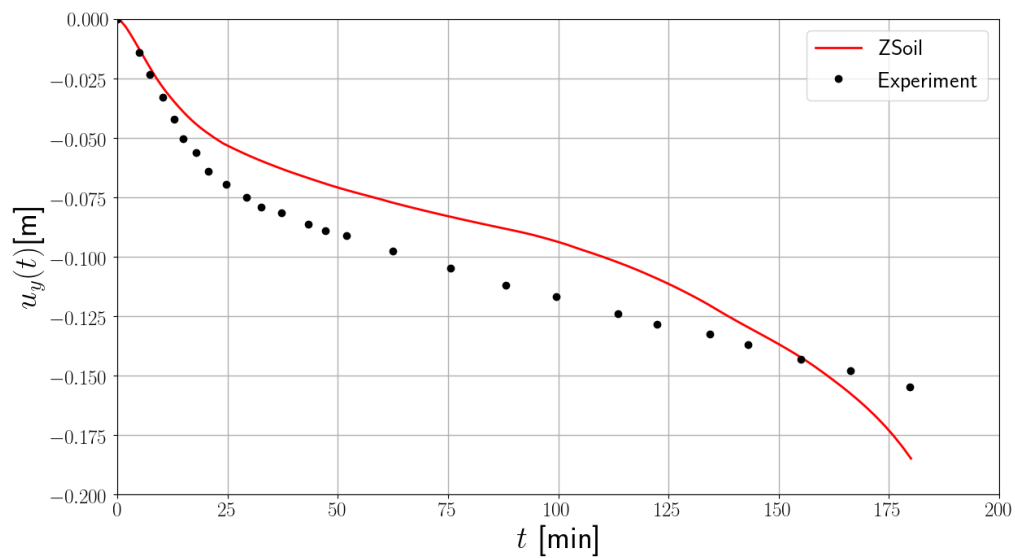


Figure 5.18: Central point deflection time history (steel strength $f_t = f_c = 500$ MPa)

5.5 Slab subject to fire conditions (Minne and Vandamme test)

Comparizon of the Minne and Vandamme (after Nechnech et al.[5]) test results, for two slabs G1 and G3 subject to fire conditions, and numerical predictions obtained with aid of modified Lee-Fenves model is the aim of this benchmark. In this test a simply supported one way rectangular slab $4.9\text{m} \times 1.9\text{m}$ (taking into account shift of supports, nominal slab dimensions are $4.5 \times 1.9\text{m}$), 150mm thick, reinforced in one direction (1178 mm^2 in slab G1 and 1414 mm^2 in slab G3), is initially loaded by the dead weight (24kN/m^3) and line loads (5.4 kN/m in slab G1 and 14.6 kN/m in slab G3), applied at distance of 1.125m from slab supports, and then subject to the fire conditions. Distance of the main reinforcement axis measured from the bottom face of the slab is 1.5cm for slab G1 and 3.5 cm for slab G3. Thermal part of this benchmark is solved with aid of Q4 continuum elements together with convection and radiation boundary conditions. In the mechanical part Q4 plane-strain elements are used. As in the plane strain we analyze unit slice in the 3-rd direction, the aforementioned reinforcement cross section area is reduced by the factor $(1.0\text{m}/1.9\text{m})$. The test setup is shown in the following figure.

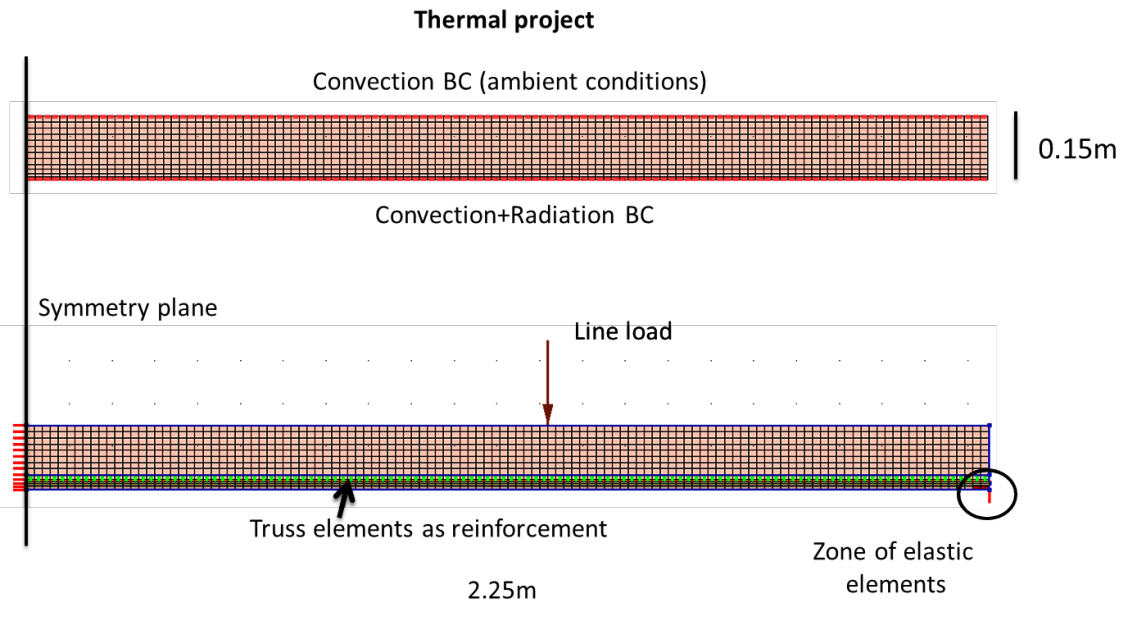


Figure 5.19: Slab subject to the fire conditions (thermal and mechanical setups)

5.5.1 Thermal analysis

Files for thermal analysis:

Fire_Minne_heat_prj.inp

Generating variable (in time) temperature field, that can later be associated with the slab is the aim of carried out thermal analysis. In this project domain is discretized with Q4 continuum elements while steel reinforcement is neglected (here we assume that steel bars have same temperature as concrete). On top of the mesh convection elements are put assuming that the ambient temperature is constant and equal to 20°C. On the bottom boundary of the mesh both convection and radiation elements are put with the ambient temperature driven by the ISO 834 fire curve ($\Theta(t) = 20 + 345 \log_{10}(8t + 1)$ (time in [min])). In this test the following set of thermal properties is used (siliceous aggregate)

Parameter	Unit	Value
λ_c	[MN/min K]	$1.17084 \cdot 10^{-4}$
c_c^*	[MJ/m ³ K]	2.160
α_c	[1/K]	$9.128 \cdot 10^{-6}$
h_c	[MN/m/min/K]	$1.5 \cdot 10^{-3}$
ϕ	[-]	1.0
ε_m	[-]	0.8
ε_f	[-]	1.0
σ	[MN/ m ³ min K ⁴]	$3.402 \cdot 10^{-12}$

Remarks:

1. Convection coefficient h_c corresponds to the EC2 recommended value 25 W/m²K

5.5.2 Mechanical analysis

Files for mechanical analysis:

Fire_Minne_mech_prj_G1.inp,

Fire_Minne_mech_prj_G3.inp

In the mechanical part of this benchmark domain is discretized with aid of Q4 plane strain elements. **Evolution functions designed for the siliceous aggregate are selected here.** Material properties of concrete are summarized in the following table.

Parameter	Unit	Value
E	[MPa]	30000
ν	[-]	0.20
\underline{f}_c	[MPa]	43.0
$\underline{f}_{co}/\underline{f}_c$	[-]	0.4
$\underline{f}_{cho}/\underline{f}_{co}$	[-]	1.16
$\underline{\sigma}_{c,D}/\underline{f}_c$	[-]	0.75
$\tilde{\sigma}_c/\underline{f}_c$	[-]	1.0

\tilde{D}_c	[-]	0.435
G_c	[MN/m]	$5 \cdot 10^{-3}$
f_t	[MPa]	2.6
$\tilde{\sigma}_t/f_t$	[-]	0.5
\tilde{D}_t	[-]	0.5
G_t	[MN/m]	10^{-4}
s	[-]	0.2
Dilatancy		Constant
α_p	[-]	0.2
α_d	[-]	1.0
Φ_{ref}	[-]	2.35

Material properties for steel reinforcement are summarized in the next table.

Parameter	Unit	Value
E	[MPa]	215000
f_t	[MPa]	500
f_c	[MPa]	500

In this benchmark secant stiffness is enforced to be used by nonlinear Newton-Raphson solver.

Central deflection time histories computed and measured for slabs G1 and G3 are shown in next two figures.

Due to plane strain conditions structural behavior is too stiff especially at later test stages (see slab G3). It has to be emphasized here that all parameters except compressive strength and Young's modulus values are taken after the EC2. No special ajustement was made to get better fit with respect to the measurements. Hence results of this benchmark have to be evaluated as good.

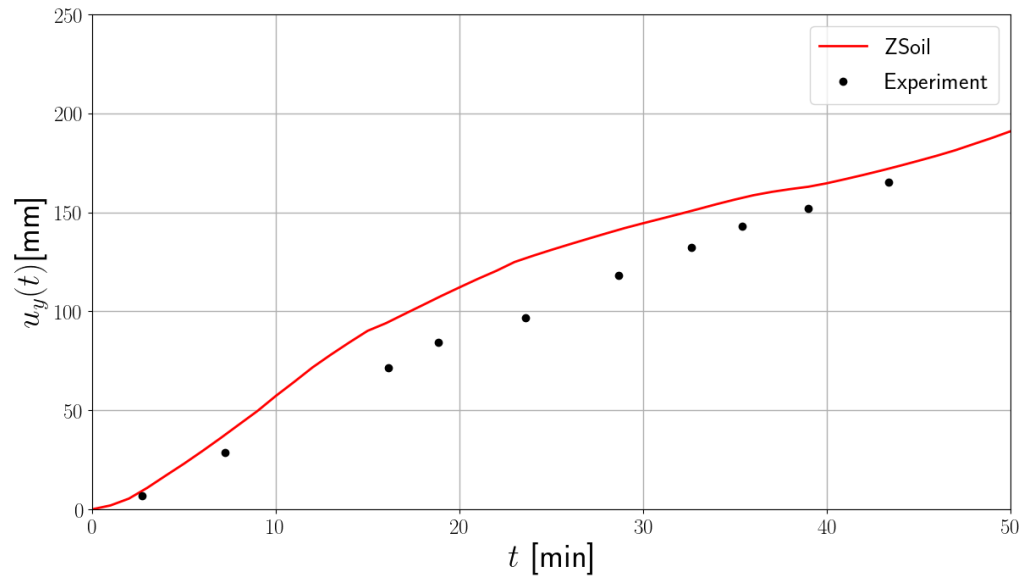


Figure 5.20: Central point deflection time history for slab G1

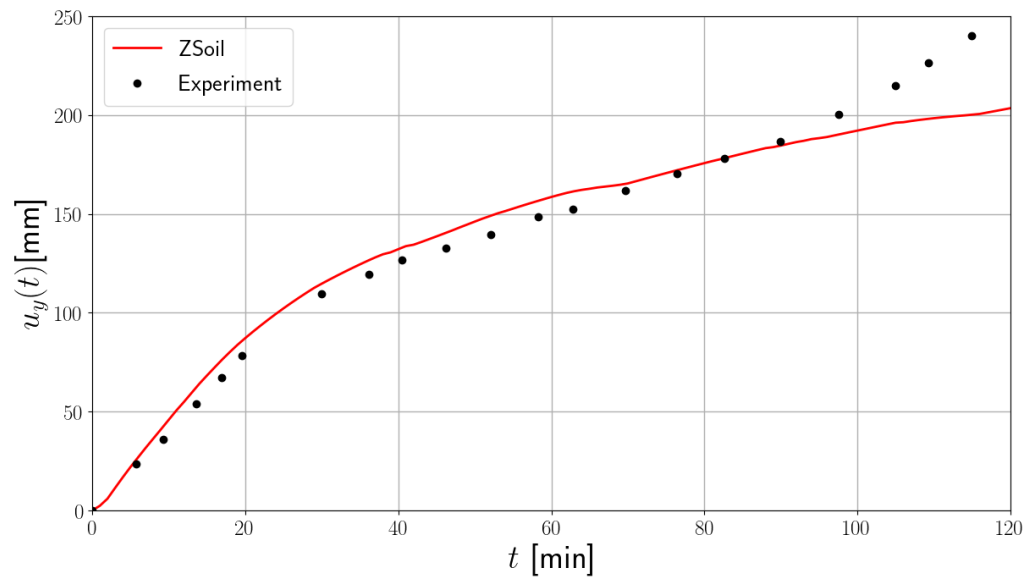


Figure 5.21: Central point deflection time history for slab G3

Bibliography

- [1] A. Truty, Th. Zimmermann.: Elastic-plastic damage model for concrete in ZSoil. Report 160102. ZACE Services Ltd.
- [2] Th. Gernay, A. Millard, J.M. Franssen. A multiaxial constitutive model for concrete in the fire situation: theoretical formulation. *Int. Journal of Solids and Structures* 50 (2013). p. 3659-3673.
- [3] Y. Anderberg, S. Thelandersson. Stress and deformation characteristics of concrete at high temperatures. 2. Experimental Investigation and material behavior model. (Bulletin of Division of Structural Mechanics and Concrete Construction, Bulletin 54; Vol. Bulletin 54). Lund Institute of Technology.
- [4] L. Lim, C. Wade. Experimental Fire Tests of Two-Way Concrete Slabs. Fire Engineering Research Report 02/12, September 2002, University of Canterbury. ISSN 1173-5996
- [5] W. Nechnech, J.M. Reynouard and F. Meftah. On the modeling of thermo-mechanical concrete for the finite element analysis of structures submitted to elevated temperatures. *Fracture Mechanics of Concrete Structures*, deBorst et al (eds), ISBN 90 2651 825 0.